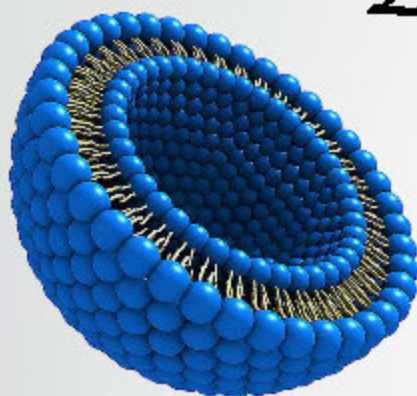


# Chapter-5

## Preparation and Characterization of Liposomes



## 5.1 Introduction

### Liposomes

Ever since the first observation by Banghan and co-workers, liposomes have been widely investigated as a promising drug delivery system for variety of hydrophobic drug molecules. Liposomes form spontaneously when certain lipids are hydrated in aqueous media (1) and range in size from a few nanometer to several micrometers in diameter. They are composed of amphiphilic lipids which are characterized by a lipophilic and hydrophilic group on the same molecule (2). As a carrier system, they consist of aqueous volume trapped by one or more bilayers of natural or synthetic lipids. Liposomal formulation is thought to be useful since due to their amenability to modifications with various molecules are easily controlled, and capability to deliver large amount of either hydrophilic or hydrophobic drugs (3) along with the property of non-toxicity, biodegradability, non-immunogenicity and biocompatibility. Depending upon their solubility and partitioning characteristics, the drug molecules are located differently in the liposomal environment and exhibit different entrapment and release properties. Hydrophobic molecules get incorporated in the bilayer of the liposomes whereas hydrophilic molecules can be accommodated in the core of the liposomes. Further, liposomes can also be formulated to encapsulate/surface conjugate genetic material. The method used for encapsulation of therapeutic agent may be either by active/remote loading or passive loading. In passive loading technique, the drug gets incorporated in the bilayer along with the lipids during film formation for hydrophobic drugs or may be loaded during hydration of lipid bilayer in the core of liposomes. But, it is generally observed that the loading efficiency achieved by passive loading is quite low and is dependent on the nature of the carrier phase and on the concentration of substance dissolved therein during hydration. However, the untrapped molecules can be subsequently recovered and reused, thus loading efficiency that is defined as amount of material encapsulated to the total amount of material involved, is not very critical. In case of hydrophilic molecule entrapment, the captured volume is an important parameter which is defined as volume of aqueous phase encapsulated in the core per unit weight of

lipids used. In the method used by Bangham et al., to the dried films obtained after evaporation of solvent in round bottom flask, hydration of lipid film was carried out by aqueous solution of drug which yield multilamellar vesicles (MLVs) spontaneously under mild agitation. The obtained MLVs can be subsequently extruded to obtain large unilamellar vesicles (LUVs) or can be probe sonicated to obtain small unilamellar vesicles (SUVs). The captured volume in case of MLVs produced by hydration is very low of the order of 2-4 $\mu$ l/mg of lipid used. To improve the entrapped volume for improving the loading efficiency, other methods that have been investigated are reverse phase evaporation, successive dehydration rehydration method or freeze thawing method.

Liposomes can enhance the therapeutic efficacy of anti-cancer agents, either by increasing the exposure of tumour cells to the drug, improving pharmacokinetic profile, decreasing the normal tissues damage, employing the enhanced permeability and retention effect (EPR) phenomenon or by utilizing the targeting principles (4).

### **PEGylated liposomes**

To achieve a higher therapeutic efficacy of administration of drug in liposomes, it is important that the liposomes along with its carrier reaches to the target site and does not distribute non-specifically to the non-target organs. The targeting approaches that are investigated fall in to two categories viz. active and passive targeting. As with most of other formulation administered systemically, for conventional liposomes also the foremost site of accumulation or screening are liver and spleen wherein reticuloendothelial system (RES) may trap them and subsequently clear them from circulation leading to an inefficacious therapeutic outcome. Passive targeting to tumour tissues takes advantage of the leaky vasculature of tumour whereby the liposomes extravasation and selectively accumulation occurs at the tumour site thus reducing the RES uptake. Passive targeting achieved by use of PEG lipid derivatives has made feasible the selective accumulation of liposomes to the tumour vasculature, by reducing RES uptake and prolonging the time for systemic circulation.

Use of PEGylated lipids is known to reduce binding of liposomes to the serum proteins thus making them invisible to the opsonisation clearance mechanism by

macrophages. Further, as a polymer it possesses biocompatibility, biodegradability, non-toxicity and non-immunogenicity that make them favourable for ease in *in-vivo* application. It is also FDA approved.

The immense importance of PEG as a conjugating ligand for pharmaceutical and biotechnology application is due to the stealth behaviour it provides to the carrier system by the following mechanism:

- Shielding the immunogenic epitopes
- Shielding receptor mediated by RES
- Prevent degradation by proteolytic enzymes

These properties confer the carrier with an increased circulation and residence time and modify the deposition characteristic. Another important aspect of PEGylation is that the PEGylated surface of liposomes can be functionalized with a variety of ligands. PEG derivatives have been designed which possess highly reactive functional sites for rapid conjugation in minimum number of steps. Variety of PEGylated proteins and peptides have become available for biopharmaceutical use and few of PEGylated products are listed: interferons (PEGasys® and Intron®), adenosine deaminase (ADAGEN®), growth hormone receptor antagonist (Somavert®), PEGasparaginase (Oncospar®), granulocyte colony stimulating factor (Neulasta®). In our research work, we have utilized DSPE-mPEG2000 as PEGylated lipid and have pre-inserted it in the liposomal membrane during film formation.

#### **PTX and its formulation:**

Present-day cancer chemotherapy with PTX is associated with hypersensitivity reactions in spite of a suitable premedication with corticosteroids and anti-histamines (5). Hence, the development of an improved delivery system for PTX is of high importance. Current approaches to the improvement are focused mainly on the development of formulations that are devoid of Cremophor EL®, investigation of the possibility of a large-scale preparation and a request for a longer-term stability. These different approaches have shown some promising possibilities to replace Taxol® by a less irritable preparation such as: (a) micelle formulations (6), (b) water-soluble prodrug preparations (7), (c) enzyme-activatable prodrug preparations conjugated with antibodies or albumin

(8, 9), (d) parenteral emulsions, (e) microspheres (10, 11), (f) cyclodextrins (12), and (g) nanocrystals (13). Figure 5.1 represents the different approaches about different formulation of PTX. Only Abraxane® (albumin nanoparticle-based PTX preparation) and Lipusu® (liposomal PTX approved by State FDA of China) have entered the field of clinical applications. Generally, liposomes and protein nanoparticles represent a promising approach to the optimization of PTX delivery. Their commercialization is at the doorstep of modern drug delivery market.

Liposomal PTX formulations are in various stages of clinical trials. LEP-ETU (NeoPharm) and EndoTAG®-1 (Medigene) have reached the phase II of the clinical trials; Lipusu® (Luye Pharma Group) has already been commercialized. The first LEP preparation was composed of EPC, cardiolipin, cholesterol, and  $\alpha$ -TAS. The liposomes were supplied as a lyophilizate by Pharmacia (Nerviano, Italy). The parameters such as MTD, recommended dose (RD), dose-limiting toxicities (DLTs), pharmacokinetics, and the anti-tumor effect of LEP were evaluated in weekly scheduled phase I study. The assessment of pharmacokinetics and the clinical data suggested that this LEP was unlikely to have any advantage over Taxol® (14). Further efforts to eliminate toxicities associated with Taxol®, to improve the drug safety profile and to enhance the PTX therapeutic efficacy led to the development of LEP formulation (marked LEP-ETU) by NeoPharm. The protection against toxicities relating to free PTX and the encouraging data regarding the tumor response enabled a successful progression of LEP-ETU into the phase II of the clinical testing for the treatment of metastatic breast cancer. The second PTX preparation was based on cationic LEP. The delivery of cationic LEP to the tumor vasculature in combination with chemotherapy affecting the proliferating tumor cells represents an effective two-component anti-tumor therapy. Generally, antiangiogenic drugs themselves cannot eradicate tumors completely. A remarkable anti-tumor effect can be achieved by combining anti-angiogenic tumor therapy with conventional cytotoxic radio- or chemo-therapy. Tumor endothelial cell apoptosis and intra-tumoral thrombosis was found to be induced by cationic LEP. This therapy supports vascular targeting as an underlying mechanism (15). This novel therapeutic strategy was first realized by the development of EndoTAG®-1 preparation by Medigene. This preparation comprised PTX encapsulated in cationic lipid complexes based on liposomes composed of

DOPC/DOTAP and the drug (molar ratio, 45/50/5) (16). EndoTAG®-1 is currently tested in the phase II of trials against various types of solid tumors. The third liposomal PTX preparation, Lipusu® (paclitaxel liposome for injection, Luye Pharma Group), was developed by Sike Pharmaceutical (Nanjing, Jiangsu, PRC). This preparation was approved by the State FDA of China. Lipusu® is the first commercially available PTX formulation to be marketed. It represents a natural extract from Yew used in the treatment of ovarian, breast, NSCLC, gastric and head and neck cancer. The application of a liposome technology resolved the issues of PTX insolubility and eliminated the use of solvents causing toxic side-effects. Abraxane® (albumin nanoparticle-bound PTX) is the only nonliposomal preparation of PTX which reached the market. The preparation was developed by Abraxis BioScience. Abraxane® was approved for the treatment of metastatic breast cancer in 2005. Albumin nanoparticle formulation allows PTX to penetrate into tumors more easily and makes the drug to be more tolerated than Taxol® (17). Abraxane® significantly improved the response rate in NSCLC patients in comparison with the generic chemotherapy by PTX drug. However, according to the data from phase III of the study, Abraxane® did not retard tumor growth or help lung cancer patients live longer (18). Hair loss, nerve pain, unusual sensations (burning or tingling), changes in the heart rhythm and weakness were side effects, even if reported in small portion of patients.

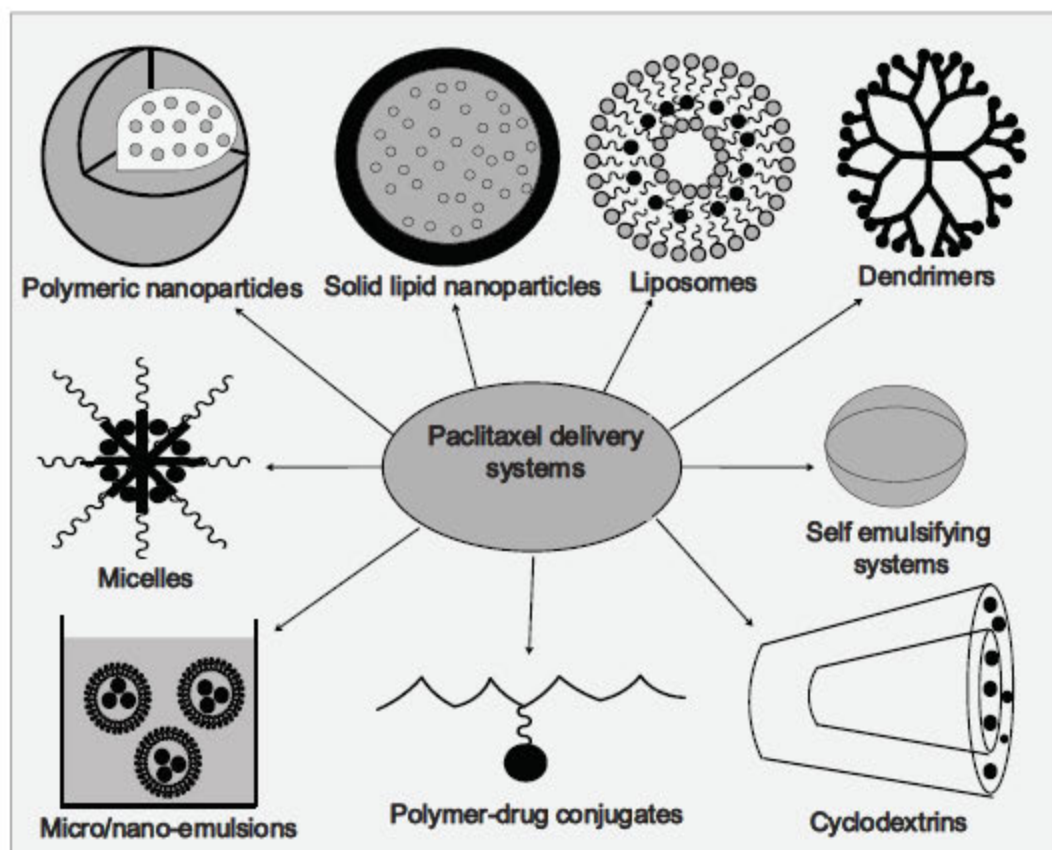


**Figure 5.1 Formulation approaches for paclitaxel**

Examples of other recently developed alternative formulations of paclitaxel that are non-cremophorylated and may preferentially target tumors include: Taxoprexin\_ is a prodrug of paclitaxel bound to the fatty acid, docosahexaenoic acid. Fatty acid cleavage occurs slowly within tumor tissues with the desired outcome of sustained tumor accumulation (19) (20). Phase II studies have demonstrated favorable results with this new paclitaxel formulation in human patients with lung melanoma and other cancers (21).

Paclical poliglumex: Paclitaxel conjugated to poly-(L-glutamic acid). This compound similarly results in drug accumulation in tumor and tumor vasculature (22). Phase II studies in nonsmall cell lung cancer, ovarian, and breast cancers are underway with encouraging early results (23).

ANG1005: Paclitaxel linked to angiopep-2 (brain peptide vector). This formulation allows paclitaxel to be transported across the blood brain barrier and to decrease active cellular efflux by evading the P-glycoprotein (Pgp) transport efflux pump

(24). This ultimately results in higher drug concentrations within the brain parenchyma after systemic delivery and a decrease in Pgp-mediated resistance.

Paccal is a novel, Cremophor-free formulation of paclitaxel. The key component of this new formulation is the use of a novel excipient composed of a surfactant-based derivative of retinoic acid (XR-17) that results in a nanoparticle micellar preparation with high water solubility that eliminates the need for Cremophor (25). This Cremophor-free formulation avoids the serious hypersensitivity issues observed with Taxol and other cremophorylated taxane formulations. In addition, the nanoparticle formulation is of a size (20–40 nm diameter) that may take advantage of the enhanced permeability and retention (EPR) effect (26). The EPR effect occurs when the nanosized macromolecules evade renal clearance resulting in prolonged elimination half-lives and exploit leaky tumor vasculature, which may result in selective and specific extravasation and accumulation within the tumor tissues. Although the size and molecular characteristics of Paccal predict it to be a formulation that would yield the EPR effect, there are insufficient data to confirm the EPR effect with this specific agent.

#### **Double loaded liposomes:**

An innovative idea in delivery of PTX discussed here, takes benefit of certain properties of the drug “containers” cyclodextrins and liposomes to combine them into a single system. The concept, involves entrapment of water-soluble cyclodextrin-PTX inclusion complexes in liposomes, would allow accommodation of insoluble drugs in the aqueous phase of vesicles (Figure 1A). Cyclodextrins (CDs), a family of cyclic amylose-derived oligomers, have been successfully used as complexation agents to enhance the solubility, stability and bioavailability of drug molecules (27).

The approach of combined liposomes and CD complexes of lipophilic drugs by forming drug-in-CD-in-liposome can increase the entrapment efficiency and modulate in vivo dissociation of the drug, thereby contributing to improvements in the pharmacokinetic profile of the drugs (28), (29). Cyclodextrin liposomal drug delivery system was first used by McCormack and Gregoriadis in 1994 (30). This strategy merges the relative advantages of the two types of carrier into a single system and avoids the use

of unnecessary organic solvents in the accommodation of water-insoluble drugs in the lipid bilayer of liposomes.

Pre-encapsulation of hydrophobic drugs in cyclodextrin could improve delivery by enabling loading into liposomes. Hydrophobic drugs encapsulated in cyclodextrin, which has a hydrophobic core and hydrophilic exterior, increased drug loading into liposomes compared with hydrophobic drugs that were not encapsulated. In mouse colon cancer xenograft models, injection of liposomes loaded with encapsulated hydrophobic cancer drugs decreased tumour growth compared with empty liposomes or free drug without adverse effects. The cancer drugs had previously failed clinical testing because of toxicity issues. Next steps could include testing the platform with additional cancer therapeutics. This could potentially increase the drug to lipid mass ratio to levels above those attained by conventional drug incorporation into the lipid phase.

## 5.2 Material and Instruments

### Materials

Sr No	Chemicals/Materials	Source/Manufacturer
1.	1,2-distearoyl-sn-glycero-3-phosphoethanolamine [methoxy (polyethyleneglycol)-2000] (DSPE-mPEG2000)	Lipoid GMBH (Ludwigshafen, Germany) – Gift Sample
2.	Cholesterol (Extra pure)	Sigma-Aldrich, Mumbai, India
3.	Dialysis Membrane	Himedia lab. Pvt. Ltd., India
4.	Egg Phosphatidylcholine (EPC)	Lipoid GMBH (Ludwigshafen, Germany) – Gift Sample
5.	Fully Hydrogenated Soya Phosphatidylcholine (HSPC)	Lipoid GMBH (Ludwigshafen, Germany) – Gift Sample
6.	Paclitaxel	Sun Pharmaceutical Industries. Ltd. (Vadodara, India) – Gift sample
7.	Sephadex G-50	Himedia lab. Pvt. Ltd., Mumbai, India
8.	Sucrose	Himedia lab. Pvt. Ltd., India

**Instruments**

<b>Sr No</b>	<b>Instruments</b>	<b>Company</b>
1.	Bath Sonicator	Sartorius, India
2.	Centrifuge	Remi Sci. Equipment, India
3.	CRYO-Transmission Electron Microscope	TECNAI G2 Spirit BioT WIN, FEI-Netherlands
4.	Deep Freezer	EIE Inst. Ltd., Ahmedabad
5.	Differential Scanning Colorimetry	Schimadzu, India
6.	Infrared (IR) Spectroscopy	Bruker,
7.	Karl-Fischer Auto titrator	Toshiwal Inst. Pvt. Ltd., India
8.	Lyophilizer	Virtis-Advantage plus, USA
9.	Magnetic Stirrer	Remi Sci. Equipment, India
10.	pH Meter	Labindia Inst Pvt. Ltd., India
11.	Shaker Incubator	Scigenic ORBITEK, Germany
12.	UV Visible Spectrophotometer	Schimadzu, India
13.	Weighing Balance	Schimadzu, India
14.	Zetasizer (Nano ZS)	Malvern Instruments, Malvern, UK
15.	RP-HPLC	Shimadzu LC-20AT, Japan
16.	Rotary evaporator	Rotavapor RV-10, IKA® India Private Limited
17.	Centrifuge (CPR-30)	Remi Elektrotechnik Ltd., Vasai, India

## 5.3 Methods

### 5.3.1 Preparation of conventional liposomes (CLs) by thin film hydration method

Conventional liposomes (CLs) containing PTX were prepared by thin-film hydration method (31). Lipid mixture containing HSPC, Egg PC and Cholesterol (different molar ratios) along with PTX (2 mg) were accurately weighed and dissolved in solvent mixture containing chloroform and methanol mixture (2:1 v/v) in a round bottom flask. The flask was connected to rotary flask evaporator and solvent was evaporated by rotary evaporator (IKA Rotavapor RV-10, IKA® India Private Limited) under vacuum for 30 min at 120 rpm in a thermo-stated water bath at temperature of  $45^{\circ}\text{C}\pm 1^{\circ}\text{C}$  to form dry lipid film. The flask was kept overnight under vacuum to remove the traces of residual solvent present in the film. The lipid film was then hydrated with filtered double distilled water for 40 min at  $55^{\circ}\text{C}\pm 1^{\circ}\text{C}$  and 100 rpm. After hydration, the liposomal suspension was transferred to a volumetric flask and volume was made till 3 ml with filtered double distilled water. Blank liposomes not containing PTX were also prepared using the above method to act as control during the cellular activity evaluation. To separate the untrapped drug from the liposomal suspension, centrifugation was carried out at 3000 rpm for 10 min at room temperature and the supernatant was taken in a stoppered glass vial. Extrusion of the hydrated liposomal suspension was carried out using 400 nm membrane filters at  $50^{\circ}\text{C}$  for 8 times followed by extrusion through 100 nm filter for 5 times. The liposomes were stored at  $2-8^{\circ}\text{C}$ .

#### *Optimization of formulation variables by D-optimal factorial design*

Liposomal formulation was optimized using D-optimal design with total 19 runs among which 6 model points were for preselected quadratic model, 5 points to estimate the lack of fit, 5 replicate points and additional 3 center points to evaluate for curvature and to estimate the pure error. From the results of optimum batch observed in preliminary screening, molar concentration of mPEG<sub>2000</sub>-DSPE was kept constant at 5 mole% in experimental design for all batches while varying the mole% of other lipids i.e. HSPC, EggPC and Chol. Variables chosen for optimization are shown in Table 5.1. Coded and

actual values used in formulation optimization are tabulated here (Table 5.2). The design was also constrained so as to keep total molar concentration of three chosen lipids to be 95 mole% in every combination. Additionally, other process and formulation parameter were kept constant during optimization.

**Table 5.1 Various variables and responses involved in optimization**

Variables	HSPC (mole%)
	EPC (mole%)
	Chol (mole%)
Response Parameter	Particle size (nm)
	Entrapment efficiency (%)

**Table 5.2 Coded and actual levels of HSPC, EPC and Chol used in optimization**

Coded levels	Actual levels		
	A: HSPC (mole%)	B: EPC (mole%)	C: Chol (mole%)
Lower (-1)	20.0	30.0	20.0
Higher (+1)	30.0	50.0	40.0
Constraint	A+B+C = 95.0 mole%		

Response surface modelling was applied using Design Expert 7.0 (Stat-Ease Inc., MN). Using multiple linear regression analysis (MLRA), different polynomial equations were evaluated for best fitting to the experimental data by determining the values of coefficients in the polynomial equations and a full and reduced model was established. Statistical soundness of the established model was checked by ANOVA statistics (32-38).

Based on the established model three-dimensional (3D) response surface plots were constructed by Design Expert Software. The 3D surface plots were useful in establishing the main effects (effect of individual variables) on the response parameter and also to have an insight to the combined effects of two variables (39-41).

Validation of the employed experimental design and chosen model for its prediction capability for the optimization of the variables was done by performing check-point analysis. Eight optimum checkpoints were selected, prepared and evaluated for response parameters. Statistical comparison between the predicted values and average of

three experimental values of the response parameters was performed to derive percentage error and to evaluate significant difference between these values. Optimum formulation parameters were selected based on the specified goal i.e. particle size and entrapment efficiency.

Optimized formulation was derived by specifying goal and importance to the formulation variables and response parameters. Results obtained from the software were further verified by actual preparation of the batches and comparing the predicted and actual results.

### ***Optimization of process variables***

After optimization of formulation using D-optimal design, the optimized formulation was subjected to challenge in processing conditions to determine the impact of process variables such as hydration time, hydration temperature and number of extrusion cycles on the entrapment efficiency and particle size of the prepared conventional liposomes. Here also, all other formulation parameters were kept constant and the processing variables were varied one by one to evaluate their impact of finished formulation characteristic.

### **5.3.2 Preparation of PEGylated conventional liposomes (PLs)**

Essentially the same processing parameter along with the composition of the optimized batch was selected for carrying out PEGylation of the liposomes. Herein, to determine the effect of amount of PEGylated lipids on the formulation characteristic, four different concentration of PEGylated lipid was screened. An amount of 1 mol%, 3 mol%, 5 mol% and 7 mol% of DSPE mPEG 2000 lipid was incorporated during preparation of dry lipid films. An equivalent amount of mole% of HSPC was decreased to compensate for the incorporation of PEGylated lipid. The technique employed was thus pre-insertion during thin film hydration. The formulations were evaluated for steric stability using invitro test along with determination of pH, particle size, zeta potential of liposomes and entrapment efficiency of drug in liposomes.

### 5.3.3 Preparation of Double loaded PEGylated liposomes (DLPLs)

Double loaded PEGylated liposomes containing paclitaxel were prepared by thin-film hydration method as stated in preparation of conventional liposomes. Lipid mixture containing HSPC, Egg PC, Cholesterol and DSPE mPEG2000 (molar ratio of 0.22:0.43:0.30:0.05) along with PTX (2 mg) were accurately weighed and dissolved in solvent mixture containing chloroform and methanol mixture (2:1 v/v) in a round bottom flask. Drug:lipid molar ratio was 1:30. The solvent was removed by rotary evaporator (IKA Rotavapor RV-10, IKA® India Private Limited) under reduced pressure for 30 min at 45°C to form dry lipid film. The flask was kept overnight under vacuum to remove the residual solvent. The dried lipid films were then hydrated by adding 3 ml of PTX-DM $\beta$ CD (PTX equivalent to 2 mg/ml) ICs at 55°C for 40 min and 100 rpm in rotary evaporator. The untrapped PTX was separated by centrifugation at 3000 rpm for 10 min. For size reduction, liposomal suspension was sequentially extruded through 400 nm polycarbonate membrane at 50°C for 8 times followed by 100 nm membrane filter for 5 times. Untrapped PTX inclusion complex was separated by Sephadex G 50 column. Both the above PLs and DLPLs dispersion were lyophilized (Virtis Advantage plus lyophilizer) using sucrose (20% w/v) as cryoprotectant and stored in sealed vials at RT and 2-8°C for stability study.

### 5.3.4 Characterization of PEGylated conventional and double loaded liposomes

#### 5.3.4.1 Particle size analysis

Particle size of liposomes was determined using principle of dynamic light scattering using Malvern Zetasizer Nano (Nano ZS, Malvern Instruments, UK). Light source was 633 nm He-Ne laser and scattering angle was 175°. Analyses were carried out at 25°C temperature after diluting 0.2 ml of formulation to 2 ml using filtered double distilled water. The total number of sub-runs for measurement of size were 15 and each run was for a duration of 10 seconds. The results were reported as Z-average along with polydispersity index after carrying out analysis in triplicate. A homogenous sample is

represented by a PDI close to 0.00 while a highly polydisperse sample has a PDI close to 1.00.

#### 5.3.4.2 Zeta potential analysis

Zeta potential values were obtained using Smoluchowski equation which takes into account electrophoretic mobility of the particles and  $175^\circ$  back-scatter. A 0.2 ml of volume of liposomes were diluted up to 2 ml with double distilled water and analysis was carried out in triplicate using zeta cuvette at  $25^\circ\text{C}$ . The measurements were done using ZetaSizer NanoZS (Malvern Instruments Ltd., UK) in triplicate.

#### 5.3.4.3 Entrapment efficiency and drug loading

For determination of entrapment efficiency, the PLs were collected and centrifuged at 3000 rpm for 10 min at  $25^\circ\text{C}$  to separate the untrapped drug. The entrapment efficiency of DLPLs was determined by passing the liposomes through Sephadex G50 gel column to separate the untrapped water soluble ICs of PTX. The liposomal fraction was treated with methanol to extract the loaded drug and was analyzed by RP-HPLC method (42). The concentration of drug in the liposomal fraction was obtained by substituting the values of mean area obtained in the standard calibration curve as reported in the analytical chapter. Similarly, entrapment efficiency of lyophilized PEGylated liposomal formulations was also determined after reconstitution and filtering the reconstituted formulation through  $0.45\mu\text{m}$  filter to obtain clear solution free from any precipitates. For determination of percentage entrapment of drug in liposomes following equation was used:

$$\% \text{ Entrapment efficiency} = \frac{\text{Actual amount of drug loaded in liposomes}}{\text{Actual amount of drug used for liposomal preparation}} \times 100$$

For determination of loading efficiency of liposomes following equation was used:

$$\% \text{ Loading Efficiency} = \frac{\text{Amount of PTX in liposomes}}{\text{Total amount of Liposomes}} \times 100$$

#### 5.3.4.4. Cryo-TEM

Morphology and size of liposomes were evaluated using Transmission Electron Microscopy (TECNAI G2 Spirit BioT WIN, FEI-Netherlands) operating at 200 kV with 0.27 nm resolution. The hydrophobic grid was converted into hydrophilic by glow discharge. The samples were spread on grid and cryo-frozen in liquid ethane at -180°C. The grid was inserted into microscope using a cryo holder and images were taken at 70,000X magnification.

#### 5.3.4.5 In vitro drug release

The release of PTX from PLs and DLPLs was investigated at  $37^{\circ} \pm 0.5^{\circ} \text{C}$  and was compared with Taxol®. Briefly, Taxol® and PLs containing equivalent amount of PTX (1 mg/ml) were placed in dialysis tubes (MWCO 12000 Da) and tightly sealed. Then, the dialysis tubes were immersed in 100 ml of release medium PBS (pH 7.4) containing 0.1% (v/v) Tween 80 (43) (44). Release medium was stirred at 150 rpm and the samples (0.5 mL) were withdrawn at 0.25, 0.5, 1, 2, 4, 8, 12 and 24 hr. The volume was made up after each sampling with fresh release medium. The sample was filtered through 0.22  $\mu\text{m}$  syringe filter and concentration of PTX was determined by RP-HPLC after appropriate dilution with methanol followed by mobile phase. The *in vitro* release experiments were conducted in triplicate for all the formulations and results were reported as cumulative amount of drug released at each time point.

#### 5.3.5 Additional characterization for PEGylated double loaded liposomes (DLPLs)

##### 5.3.5.1 DSC and FTIR

Differential scanning calorimetry was carried out for plain Paclitaxel, physical mixture of lipids and paclitaxel and prepared DLPLs. Approximately 3-5 mg of each sample was placed in aluminum pans and DSC was carried out against empty aluminum pan as reference. Heating scans by heat runs for each sample was set from 30 °C to 300 °C at 10 °C/ min in a nitrogen atmosphere.

Plain Paclitaxel, physical mixture and DLPLs were investigated using Fourier transform infrared spectrophotometer/FTIR (Bruker, Germany) range between 4000 and 400  $\text{cm}^{-1}$ , with a resolution of 2  $\text{cm}^{-1}$ . All powder samples were compressed into KBr disks for the FTIR measurement.

### **5.3.5.2 Olympus microscopy**

Optimal microscopy of the prepared liposomes were carried out to evaluate its morphology. A drop of DLPLs were placed on glass slide and covered with cover slip and observed under Optical microscope at 40X magnification.

### **5.3.5.3 Sodium sulphate induced flocculation or electrolyte induced flocculation study**

Solution of sodium sulphate ranging in molarity from 0.0 M to 1.0 M viz. 0.0 (double distilled water) 0.2, 0.4, 0.6, 0.8 and 1.0 M were prepared and to 4 ml of this solution, 1 ml of PEGylated liposomes prepared with varying mol% of DSPE mPEG-2000 lipid were incubated for a period of 2 hours. Incubation was carried out in a shaker incubator at 37°C. To determine the flocculation in liposomal suspension induced by presence of electrolytes, the % transmittance of the mixture after incubation was measured at 630 nm using UV-Visible spectrophotometer. The transmittance values were converted to absorbance using the equation: Absorbance = 2-log(%T). Further, the impact of electrolyte challenge on liposomes were also assessed by measuring the particle size and zeta potential.

### **5.3.5.4 In vitro serum protein adsorption/ opsonisation study**

#### **5.3.5.4.1 In vitro serum/liposome incubation**

200 $\mu\text{l}$  of both conventional and PEGylated liposomal suspension were taken in 1.5 ml Eppendorf tubes. The volume was made up to 1000  $\mu\text{l}$  with 100% Fetal Bovine Serum (FBS) so as to achieve a final concentration of 80% FBS in the mixture. The mixture was incubated for 1 hr at 37°C in shaker incubator. After the incubation period, the tubes were immediately removed and cooled on ice bath for 5 min to prevent further interaction.

#### ***5.3.5.4.2 Isolation of liposomes from incubation mixture***

Separation of liposomes from serum proteins was carried out using Sepharose CL-4B gel column. Sepharose (5%) was hydrated in double distilled water and filled in 30 cm long column (10 ml pipette). Double distilled water was run through the column to saturate the column with the running solution. The incubation mixture was loaded on the gel column and elution was carried out using double distilled water. Fraction of 500 $\mu$ l were collected and replaced with equal amount of double distilled water. Each fraction was analyzed for content of phospholipids present in the liposomes using Stewart method with minor modification (Reference: Analytical method chapter). The liposomal fraction (typically fractions 7-10; a total volume of 2 ml) from column were combined and analyzed for size, zeta potential, amount of serum protein adsorbed as well as the lipid content. The samples were stored at -70°C till analysis.

#### ***5.3.5.4.3 Determination of % recovery of liposomes***

To determine the % recovery of liposomes, the total phospholipid content of the liposomes before incubation and after separation through gel column using a modified Stewart method.

*For recovery before incubation with serum:* 200 $\mu$ l of liposomal suspension was taken in 1.5 ml Eppendorf tubes and to it double distilled water was added to make up the volume to 1 ml. To 0.1 ml of above diluted liposomal dispersion, 3 ml each of chloroform and ammonium ferrothiocyanate solution was added.

*For recovery after incubation of serum:* To 200 $\mu$ l of liposomal suspension collected after pooling the fractions, 3 ml each of chloroform and ammonium ferrothiocyanate solution was added and vortexed vigorously for 2 minutes.

Both the above samples of liposomes in biphasic mixture was allowed to separate, and the lower chloroform fraction containing lipid was analyzed in UV visible spectrophotometer at  $\lambda_{max}$  of 472 nm using chloroform blank. The amount of lipid was estimated using the calibration curve.

The percentage recovery of liposomes was determined using the following equation:

$$\% \text{ Liposome recovery} = \frac{\text{Total lipid amount recovered from liposomes}}{\text{Total lipid amount in the incubated liposomal dispersion}} \times 100$$

#### ***5.3.5.4.4 Determination of mean particle size and zeta potential***

To investigate the impact of serum adsorption on physical parameters of liposomal dispersion, particle size and zeta potential measurement of the liposomes before and after incubation with serum was carried out.

#### ***5.3.5.4.5 Estimation of total serum proteins associated with recovered liposomes***

BCA protein assay kit was used for quantification of proteins associated with the liposomes after incubation with serum. It was confirmed that the presence of lipid in the sample did not cause interference with the assay method in the experiment. Bovine serum albumin was taken as standard and calibration curve was generated against which the concentration of protein in the test sample was determined using UV visible spectrophotometer. The wavelength maximum was 562 nm. The amount of proteins bound to the liposomes or the protein binding index was calculated by taking ratio of the amount of total protein (gm) to the total lipid (mole) in the liposomes as described by Chonn et al. 1992. The method employed is stated briefly here. To 200µl of recovered liposomal suspension, 1.8 ml of methanol was added to extract the lipids in 2 ml Eppendorf tubes. The above extract was evaporated on a water bath maintained at 50°C to remove methanol and obtain dry residue. 1 ml of double distilled water was added to the above obtained residue and mixed thoroughly and sonicated in bath sonicator for 1 minute to disperse the residue. Centrifugation was carried out at 6000 rpm for 10 min to sediment the residual lipids. A 0.05% w/v solution of sodium azide (160µl) was added to 40µl of supernatant obtained after centrifugation. To the above reaction mixture, 2 ml of BCA working reagent was added and incubated at 60°C for half an hour. Finally, the tubes were kept in cooled condition to prevent further reaction and absorbance of the resulting solution was measured at 562nm using double distilled water as blank.

### 5.3.5.5 Liposome membrane integrity test

To investigate the intactness of liposomal membrane upon entrapment of PTX either encapsulated in the bilayer or as complex with DM $\beta$ CD and also after double loading, membrane integrity test was performed. For the test, 5,6-carboxyfluorescein (CF), a highly hydrophilic dye was encapsulated in liposomes. The test was carried out according to the method indicated by Fatouros et al. 26. Briefly, during preparation of liposomal vesicles, CF was encapsulated in hydration media at a concentration of 100  $\mu$ M. The prepared liposomes were incubated with fetal bovine serum at 37 °C at 1:5 volume ratio. Incubation was carried out for a period of 24 hr and samples were withdrawn. Percentage retention of CF fluorescence was analyzed after suitable dilution with tris buffer (pH 7.4) prior to and post liposomal membrane disruption (by 1% triton X 100). Excitation and emission wavelength for the measurement were 520 nm and 470 nm respectively. For comparison purpose, empty liposomes and plain DM $\beta$ CD in liposomes were also tested. Control measurements were made to rule out the possible interaction of CF with cyclodextrin.

The percent of CF latency was determined at each time point using the equation:

$$\% \text{ Latency} = (FI_{\text{total}} - FI_{\text{initial}}) / (FI_{\text{total}}) \times 100$$

where  $FI_{\text{initial}}$  and  $FI_{\text{total}}$  are the CF fluorescence intensities of each sample in the absence and presence of 1% Triton X-100, respectively. The CF retained in liposomes (% retention) was determined by considering the initial latency of CF.

### 5.3.6 Lyophilization of PLs and DLPLs

The PEGylated conventional liposomes and double loaded liposomes were lyophilized to impart long term physical stability to the formulation. Different quantities of cryoprotectant were screened to evaluate its effect on the liposomal formulation characteristic such as particle size and drug content. The prepared PEGylated liposomes and DLPLs were diluted in filtered double distilled water containing cryoprotectant to obtain desired concentration of the drug prior to lyophilization. The formulations were

filled in 10 ml of USP type 1 glass vials (Schott-Kaisha Pvt. Ltd., Maharashtra, India). Half stoppering of vials was done with stoppers made of chlorobutyl rubber (Helvoet, Belgium) to allow sublimed ice to escape during primary and secondary drying stage of the lyophilization cycle. The lyophilization was carried out in Virtis Advantage-Plus, SP Scientific, USA with temperature probe inserted in the vials to record the thermal processing stages of sample during lyophilization process. Freezing of the liposomes was carried out at  $-40^{\circ}\text{C}$  under vacuum of 100 mTorr. A detailed setup of the lyophilization steps and parameters is provided in the Table 5.3. Figure 5.2 represents the lyophilization cycle for the product. After lyophilization, the formulations were tightly stoppered and vials were stored under refrigerated condition until further use.

**Table 5.3 Lyophilization cycle**

Freezing: $-40^{\circ}\text{C}$ ; Vacuum: 200 mTorr; Condenser: $-60^{\circ}\text{C}$							
Thermal Treatment steps				Primary drying			
Step	Time	Temp.	Ramp/ Hold (R/H)	Temp.	Time	Vacuum	R/H
1	5	30	R	-40	360	100	H
2	-5	30	R	-25	30	100	R
3	-5	60	H	-25	120	100	H
4	-40	70	R	-10	30	100	R
5	-40	260	H	-10	30	100	H
6	-	-	-	0	20	100	R
7	-	-	-	0	30	100	H
8	-	-	-	10	20	100	R
9	-	-	-	10	30	100	H
10	-	-	-	25	45	100	R
11	-	-	-	25	120	100	H
12	-	-	-	-	-	-	-
Post Heat				25	600	100	-

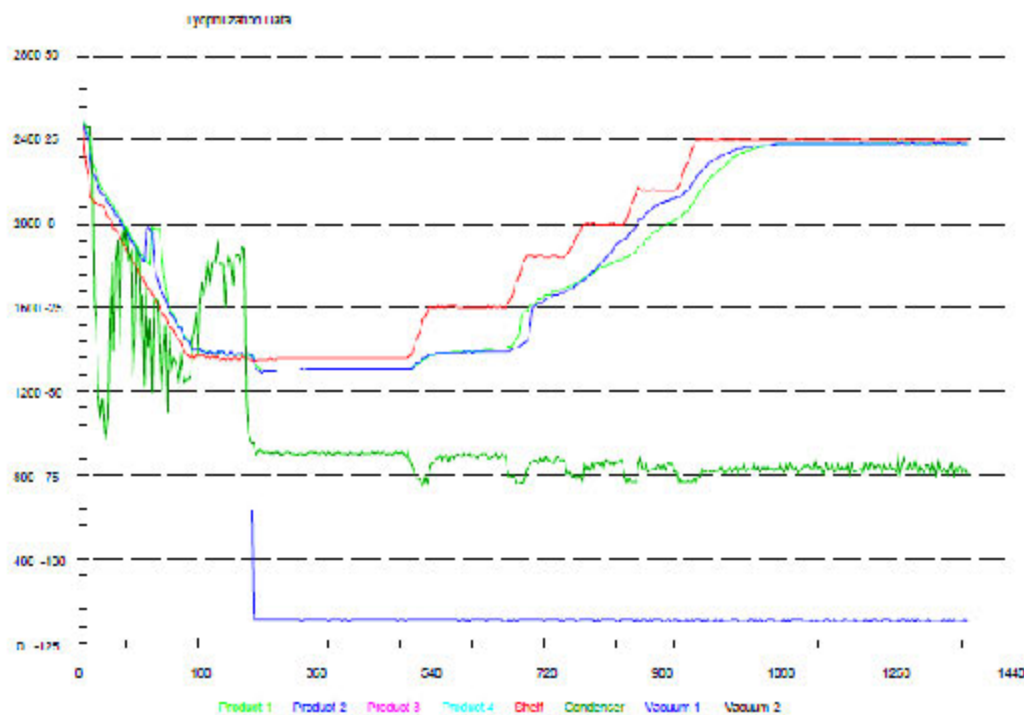


**Figure 5.2 Thermal changes during Lyophilization of Liposomes**

### 5.3.7 Stability Studies

Stability study of any formulation on storage is necessary as it reflects whether the desirable properties of the formulation are retained on storage (45, 46). These desirable properties include integrity of lipid vesicles and size distribution of particles. Upon storage, liposomes are susceptible to many physical changes i.e. lipid particles may undergo fusion and aggregation leading to increase in particle size of liposomes. Also there may occur loss of integrity of liposomes and subsequently leakage of encapsulated drug may take place (47, 48). Liposomal formulations are not stable enough in an aqueous dispersion form. So, to increase their stability the liposomal formulations are freeze-dried (lyophilized). However, during lyophilization the liposomal formulation may undergo aforementioned physical changes. To avoid such changes different lyoprotectants like sucrose, mannitol, glycerol, trehalose, povidone, dextran etc. can be used which maintain the product in a good state (49, 50). The physical testing of such product should be carried out to check whether any changes take place in the liposomal product in terms of its particle size and entrapment efficiency. So after storage period, the

liposomal formulation, on rehydration, should retain the same characteristics it possessed before lyophilization. For liposomal products an attention has been focused on two processes affecting the quality and therefore acceptability of liposomes (51). First leakage of entrapped molecules from the vesicles may take place into the extra liposomal compartment. Secondly, there is a possibility of liposomal aggregation and/or fusion, which leads to formation of larger particles (52-55). Although under dehydrated storage, there is least possibility of the formulation to encounter hydrolytic degradation. Another aspect to be considered is liposome oxidation (56).

As per the ICH stability study guideline Q1A (R2), stability studies should be performed on a drug product intended for storage in refrigerator at following storage conditions. (Table 5.4) The stability protocol was designed as per ICH guidelines (57) for countries falling under zone III (hot, dry) and zone IV (very hot, humid) (58); however, only short term studies for 3 months storage period were performed for having the idea of the stability of the product.

**Table 5.4 Stability Testing Conditions for Drug Product Intended for Storage in Refrigerator as per ICH Guideline Q1A(R2).**

Study	Storage condition	Time period for which study should be carried out
Long term	5°C ± 3°C	12 months
Accelerated	25°C ± 2°C/60% RH ± 5% RH	6 months

Any “significant change” for a drug product is defined as:

1. A 5% change in assay from its initial value; or failure to meet the acceptance criteria for potency when using biological or immunological procedures;
2. Any degradation product’s exceeding its acceptance criterion;
3. Failure to meet the acceptance criteria for appearance, physical attributes, and functionality test (e.g., color, phase separation, resuspendibility, caking, hardness, dose delivery per actuation); however, some changes in physical attributes (e.g.,

softening of suppositories, melting of creams) may be expected under accelerated conditions;

4. Failure to meet the acceptance criterion for pH;
5. Failure to meet the acceptance criteria for dissolution for 12 dosage units.

## **Method**

Stability study for the DLPLs suspension and lyophilized product after reconstitution with double distilled water was performed at storage conditions of  $25^{\circ}\pm 2^{\circ}\text{C}/60\%\pm 5\% \text{RH}$  and at  $2-8^{\circ}\text{C}$  for three months. At different time point formulations were evaluated for particle size and % drug retained. Lyophilized formulations in Type I tubular glass vials were sealed with chlorobutyl rubber stoppers and sealed with aluminum seals. Sealed vials were stored at above mentioned condition (59-66). At each sampling point different vials were used for the stability testing. The DLPL formulations were examined visually for the evidence of discoloration. The content of the vials were tested for particle size, zeta-potential, assay and water content.

### **5.3.8 Statistical Analysis**

All analyses were performed in triplicate and data are represented as mean $\pm$ standard deviation, unless otherwise mentioned. Statistical data analysis was performed using ANOVA and Student's t-test. GraphPad Prism (version 6, USA) was used for all analyses and p value  $< 0.05$  was considered significant.

## 5.4 Result and Discussion

### 5.4.1 Preparation of conventional liposomes

Initially, optimization of Drug to Lipid ratio was carried out to achieve the highest entrapment of PTX in lipid bilayer with considerable size. Amongst the ratios tried (Drug:Lipid; 1:20, 1:30 and 1:40) the 1:30 ratio was optimized based on its highest entrapment efficiency. The summary of various optimization steps for the conventional liposomes using D-optimal design are presented herein.

#### a) Design Matrix

19 batches of liposomes were prepared using composition depicted in the design matrix in Table 5.5. All formulations were evaluated for particle size and % Entrapment Efficiency (%EE) and the results obtained are shown in Table 5.5. All experiments were replicated three times and mean values of experiments were fed to the design matrix for statistical evaluation.

**Table 5.5 Design Matrix for PEGylated Paclitaxel Loaded Liposome Optimization**

Std Run	Exp Run	Factor 1 A:HSPC mole%	Factor 2 B:EPC mole%	Factor 3 C:Chol mole%	Response 1 Mean Particle Size nm	Response 2 % EE
6	1	25.6	39.6	29.8	154.6	91.95
2	2	22.2	50.0	22.8	110.3	94.45
17	3	30.0	30.2	34.8	250.2	67.56
3	4	30.0	30.2	34.8	245.3	69.25
15	5	22.2	50.0	22.8	101.4	97.65
9	6	30.0	34.8	30.2	206.5	75.65
14	7	25.0	40.0	30.0	161.8	90.52
16	8	23.8	31.2	40.0	279.6	45.26
18	9	30.0	43.1	21.9	144.3	94.34
13	10	25.0	40.0	30.0	150.4	92.24

1	11	30.0	43.1	21.9	133.1	91.45
19	12	20.0	37.2	37.8	231.5	62.15
7	13	20.0	37.2	37.8	227.3	67.48
8	14	23.3	44.9	26.8	122.6	93.15
4	15	23.8	31.2	40.0	286.5	52.58
5	16	20.0	42.4	32.6	170.6	78.04
10	17	25.3	35.0	34.7	201.4	82.52
11	18	27.1	47.9	20.0	132.2	90.95
12	19	25.0	40.0	30.0	154.6	86.52

### *i. Statistical Analysis of Response 1 (Particle Size)*

#### Selection of the prediction model:

Summary of the ANOVA results for different models as shown in Table 5.6 which depicts sequential p-values and Lack of Fit p-values along with Adjusted and Predicted R-squared values for different models.

**Table 5.6 Summary of ANOVA results for Different Models**

Source	Sequential p-value	Lack of Fit p-value	R-Squared	Adjusted R-Squared	Predicted R-Squared	
Linear	< 0.0001	0.0004	0.9084	0.8970	0.8779	
Quadratic	< 0.0001	0.1372	0.9889	0.9847	0.9748	Suggested
Special Cubic	0.7986	0.1009	0.9890	0.9835	0.9563	
Cubic	0.2947	0.0795	0.9926	0.9851	0.8688	

Highest polynomial showing the lowest p value (<0.05) along with highest Lack of Fit p-value (>0.1) was considered for model selection. Based on the criteria quadratic model was found to be best fitted to the observed responses. Special cubic and higher models were not suitable for prediction either due to low R-squared values and/or due to higher p value as compared to quadratic model (Table 5.7). Quartic and higher models

were aliased indicating the confounding of the model terms by the other implying that the predicted response would give the wrong idea of the actual response.

**Table 5.7 ANOVA for Quadratic Mixture Model**

Source	Sum of Squares	df	Mean Square	F Value	p-value Prob > F	
Model	58422.56	5	11684.51	232.00	< 0.0001	Significant
<i>Linear Mixture</i>	<i>53667.88</i>	<i>2</i>	<i>26833.94</i>	<i>532.79</i>	<i>&lt; 0.0001</i>	
<i>AB</i>	<i>474.53</i>	<i>1</i>	<i>474.53</i>	<i>9.42</i>	<i>0.0090</i>	
<i>AC</i>	<i>1256.35</i>	<i>1</i>	<i>1256.35</i>	<i>24.95</i>	<i>0.0002</i>	
<i>BC</i>	<i>3954.54</i>	<i>1</i>	<i>3954.54</i>	<i>78.52</i>	<i>&lt; 0.0001</i>	
Residual	654.74	13	50.36			
<i>Lack of Fit</i>	<i>441.30</i>	<i>6</i>	<i>73.55</i>	<i>2.41</i>	<i>0.1372</i>	<i>not significant</i>
<i>Pure Error</i>	<i>213.43</i>	<i>7</i>	<i>30.49</i>			
Cor Total	59077.30	18				

The Model F-value of 232.00 implies the model is significant. There is only a 0.01 % chance that a "Model F-Value" this large could occur due to noise. Values of "Prob > F" less than 0.0500 indicate model terms are significant. In this case all main effects (A, B and C as indicated by linear mixture in the (Table 5.7) are significant model terms showing that all the chosen factors have significant effect on particle size for given set of experimental conditions. Additionally, all the factors are involved in two way interactions with each other as shown by p value <0.0001 for interaction terms AB, AC and BC. Values greater than 0.1000 indicate the model terms are not significant. The "Lack of Fit F-value" of 2.41 and Lack of Fit p value of 0.1372 infer the Lack of Fit to be not significant relative to the pure error i.e. the selected model fits effectively to the observed experimental runs and is effective in predicting responses all over the design matrix.

Table 5.8 Summary of ANOVA results for Quadratic Mixture Model

Std. Dev.	7.10	R-Squared	0.9889
Mean	182.33	Adj R-Squared	0.9847
C.V. %	3.89	Pred R-Squared	0.9748
PRESS	1488.73	Adeq Precision	43.375

Summary of ANOVA results for selected Quadratic Mixture model is shown in Table 5.8. The "Pred R-Squared" of 0.9748 is in reasonable agreement with the "Adj R-Squared" of 0.9847 i.e. difference not more than  $<0.2$ . "Adequate precision" which is a measure of the signal to noise ratio is 43.375 indicating an adequate signal for the model to be used to navigate the design space.

Effects of factors on response (particle size):

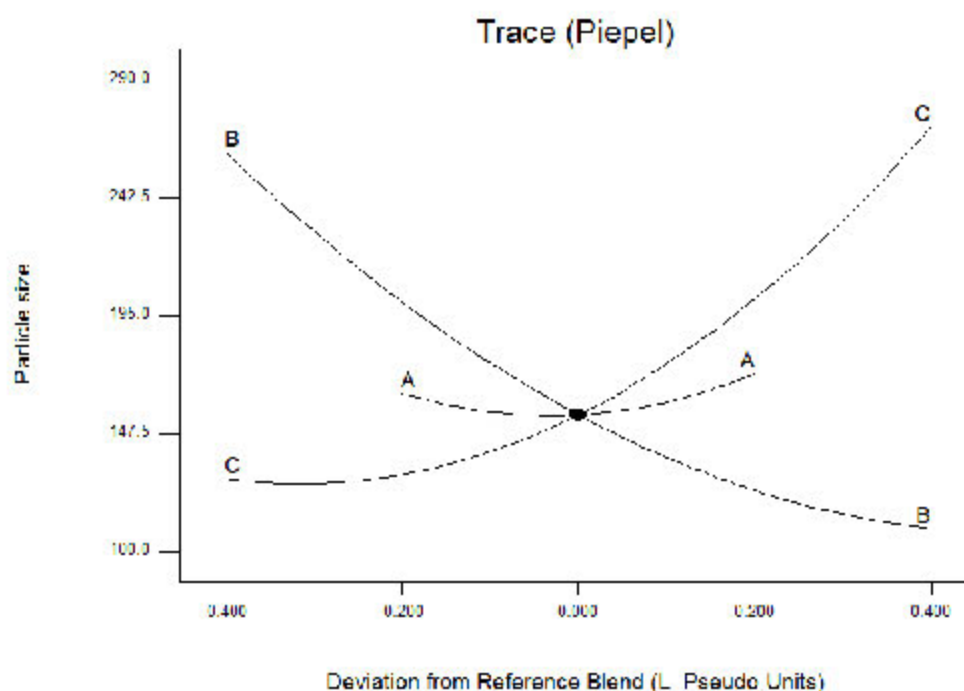
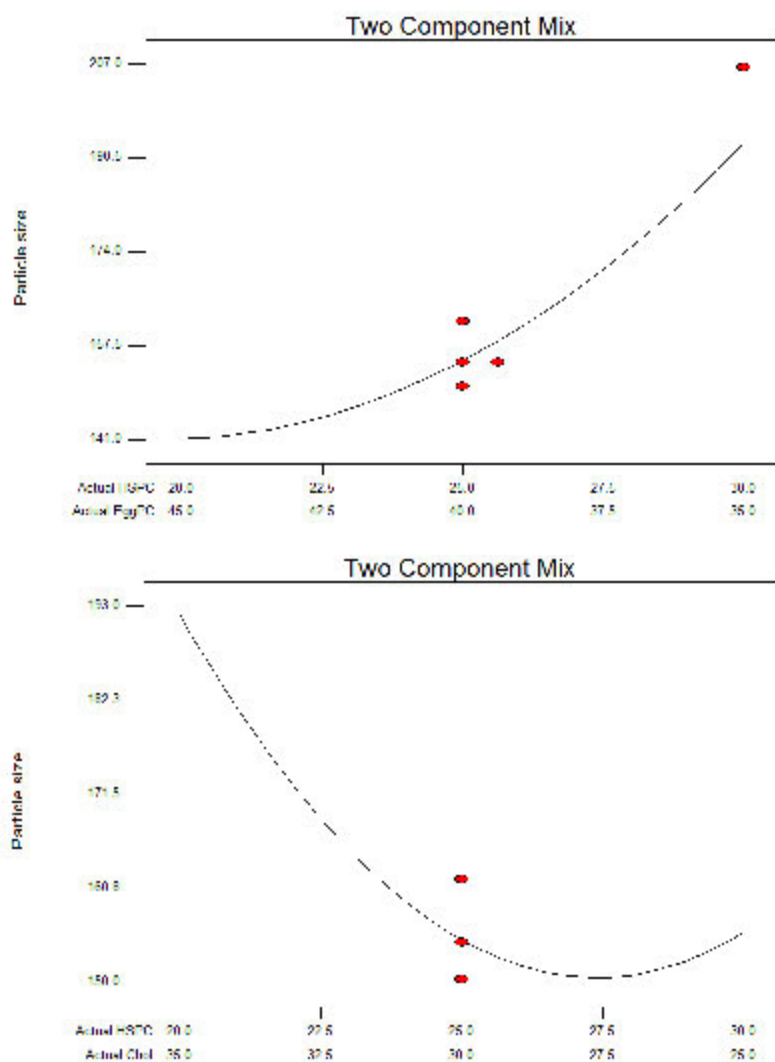
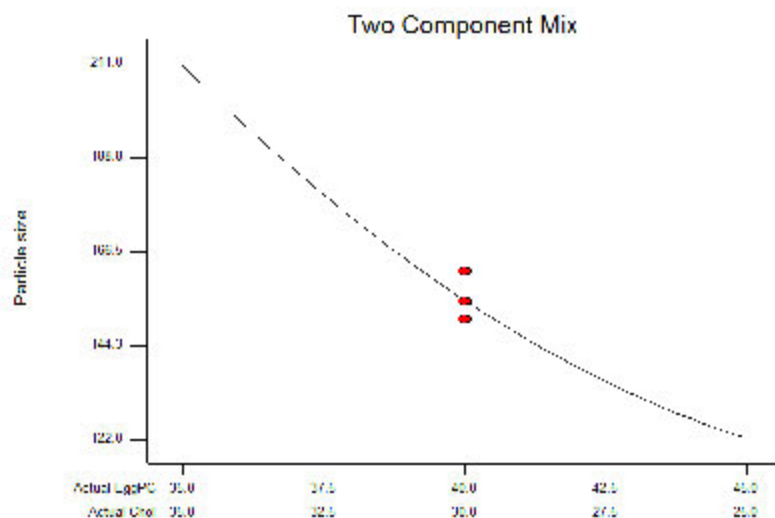


Figure 5.3 Piepel's plot (A=HSPC, B=EggPC and C=Chol)

Piepel's plot is a trace plot showing the effect of individual factors plotting the pseudo limits of one component keeping the ratio of the changeable amounts of the each components kept constant against the response. The responses are plotted as deviations

from the reference blend i.e. centroid (pseudo center point of the constrained design). As it can be seen from the plot (Figure 5.3), HSPC and cholesterol has positive effects on the particle size indicated by increase in the particle size along the increase in the mole% of these components. Cholesterol leads to increase in in a steep fashion. On the other hand, EggPC shows a negative effect on the particle size depicting steep decrease in the particle size on increasing mole% of EggPC in the mixture.





**Figure 5.4 Two-component mixture plots:- A: effect of HSPC and EPC, B: effect of HSPC and Chol, C: effect of EPC and Chol**

Two component mix plots shows (Figure 5.4) the combined effects of two components on the response keeping the value of another component kept constant at its centroid value. As it can be seen from the Table 6.63 A, as the ratio of HSPC:EPC increases i.e. mole% of HSPC increases and mole% of EPC decreases, particle size increases. This can be explained by the increasing amounts of saturated long chain fatty acyl chains of phospholipids present in the HSPC (85% DSPC and 14% DPPC) and decreasing amount of mono- and polyunsaturated phospholipids (present in the EggPC) which constitute ~49% of fatty acids in the EggPC and particularly the presence of ~40% of 1-palmitoyl-2-oleoylphosphatidylcholine (Figure 5.5) (67).

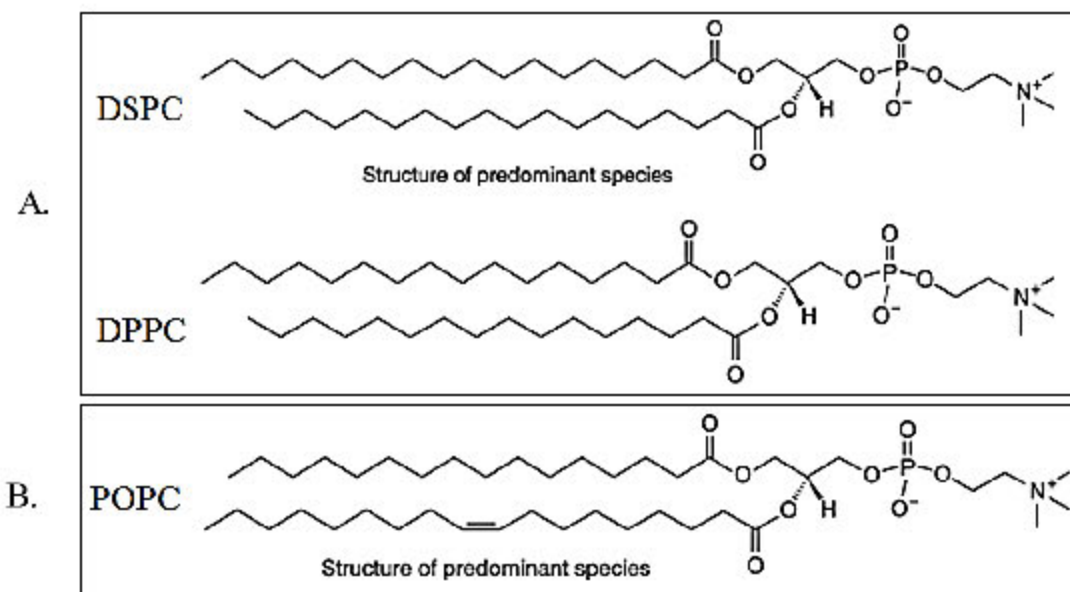


**Figure 5.5 Major lipid compositions of HSPC (A) and EggPC (B), DSPC-Distearoyl-sn-glycerophosphocholine, DPPC – Dipalmitoyl-sn-glycerophosphocholine and POPC, Palmitoyl oleoyl-sn-glycerophosphocholine**

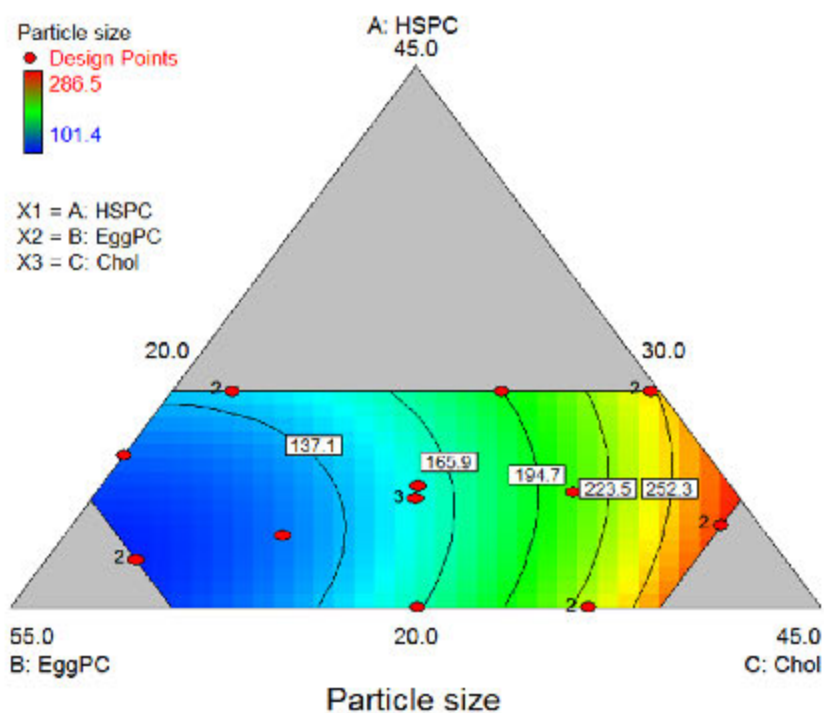


**Figure 5.6 Contour plot of effects of different components on particle size**

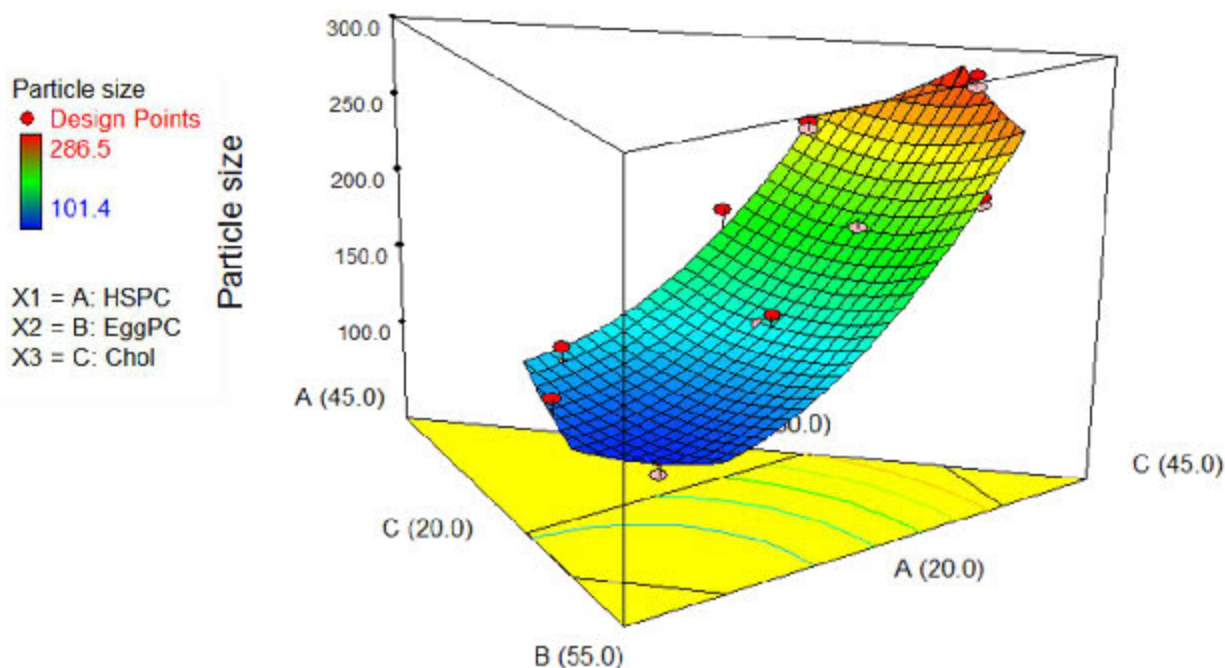


**Figure 5.7 Response surface plot of effects of different components on particle size**

Contour plot (Figure 5.6) and response surface plot (Figure 5.7) show effects of all three components on the particle size. To summarize, with increasing mole% of EggPC causes decrease in the particle size while increase in the mole% of HSPC and Cholesterol in the mixture brings about an increase in the particle size. The effects can be explained with similar justifications mentioned under the two component mix plots.

#### **Equation for prediction of particle size over design matrix**

Equation for prediction of particle size within the design matrix is given below.

$$\begin{aligned} \text{Particle size} = & \\ & +28.10030 \quad * \text{HSPC} \\ & +6.56641 \quad * \text{EggPC} \\ & +26.75510 \quad * \text{Chol} \\ & -0.48991 \quad * \text{HSPC} * \text{EggPC} \\ & -0.76037 \quad * \text{HSPC} * \text{Chol} \\ & -0.46062 \quad * \text{EggPC} * \text{Chol} \end{aligned}$$

ii. *Statistical Analysis of Response 2 (Percent Entrapment Efficiency- %EE)*

Selection of Prediction Model:

Summary of the ANOVA results for different models as shown in Table 5.9 depicts sequential p-values and Lack of Fit p-values along with Adjusted and Predicted R-squared values for different models.

**Table 5.9 Summary of ANOVA results for Different Models**

Source	Sequential p-value	Lack of Fit p-value	R- Squared	Adjusted R- Squared	Predicted R-Squared	
Linear	< 0.0001	0.0029	0.7762	0.7482	0.7039	
Quadratic	<u>0.0002</u>	<u>0.1121</u>	<u>0.9476</u>	<u>0.9274</u>	<u>0.8893</u>	Suggested
Special Cubic	0.7925	0.0817	0.9479	0.9218	0.8400	
Cubic	0.2913	0.0629	0.9649	0.9298	0.3427	

Highest polynomial showing the lowest p value (<0.05) along with highest Lack of Fit p-value (>0.1) was considered for model selection. Based on the criteria quadratic model was found to be best fit the observed responses. Special cubic and higher models were not suitable for prediction either due to low R-squared values and/or due to higher p value as compared to quadratic model. Quartic and higher models were aliased indicating the confounding of the model terms by the other implying that the predicted response would give the wrong idea of the actual response. Table 5.10 below shows the ANOVA analysis of the suggested quadratic model.

**Table 5.10 ANOVA for Quadratic Mixture Model**

Source	Sum of Squares	df	Mean Square	F Value	p-value Prob > F	
Model	4101.54	5	820.31	46.99	< 0.0001	significant
<i>Linear Mixture</i>	<i>3359.78</i>	<i>2</i>	<i>1679.89</i>	<i>96.23</i>	<i>&lt; 0.0001</i>	

<i>AB</i>	74.94	1	74.94	4.29	0.0587	
<i>AC</i>	199.54	1	199.54	11.43	0.0049	
<i>BC</i>	612.92	1	612.92	35.11	< 0.0001	
Residual	226.95	13	17.46			
<i>Lack of Fit</i>	158.00	6	26.33	2.67	0.1121	<i>not significant</i>
<i>Pure Error</i>	68.95	7	9.85			
Cor Total	4328.49	18				

The Model F-value of 46.99 implies the model is significant. There is only a 0.01 % chance that a "Model F-Value" this large could occur due to noise. Values of "Prob > F" less than 0.0500 indicate model terms are significant. In this case all main effects (A, B and C as indicated by linear mixture in the Table) are significant model terms showing that all the chosen factors have significant effect on particle size for given set of experimental conditions. Additionally, all the factors are involved in two way interactions with each other as shown by p value <0.05 for interaction terms AB, AC and BC. Values greater than 0.1000 indicate the model terms are not significant. The "Lack of Fit F-value" of 2.67 and Lack of Fit p value of 0.1121 infer the Lack of Fit to be not significant relative to the pure error i.e. the selected model fits effectively to the observed experimental results and is effective in predicting responses all over the design matrix.

**Table 5.11 Summary of ANOVA results for Quadratic Mixture Model**

<b>Std. Dev.</b>	4.18	<b>R-Squared</b>	0.9476
<b>Mean</b>	80.20	<b>Adj R-Squared</b>	0.9274
<b>C.V. %</b>	5.21	<b>Pred R-Squared</b>	0.8893
<b>PRESS</b>	479.25	<b>Adeq Precision</b>	18.545

Summary of ANOVA results for selected Quadratic Mixture model is shown in Table 5.11. The "Pred R-Squared" of 0.8893 is in reasonable agreement with the "Adj R-Squared" of 0.9274 i.e.  $<0.2$ . "Adequate precision" which is a measure of the signal to noise ratio is 18.545 indicating an adequate signal for the model to be used to navigate the design space.

#### Effect of factors on response (EE)

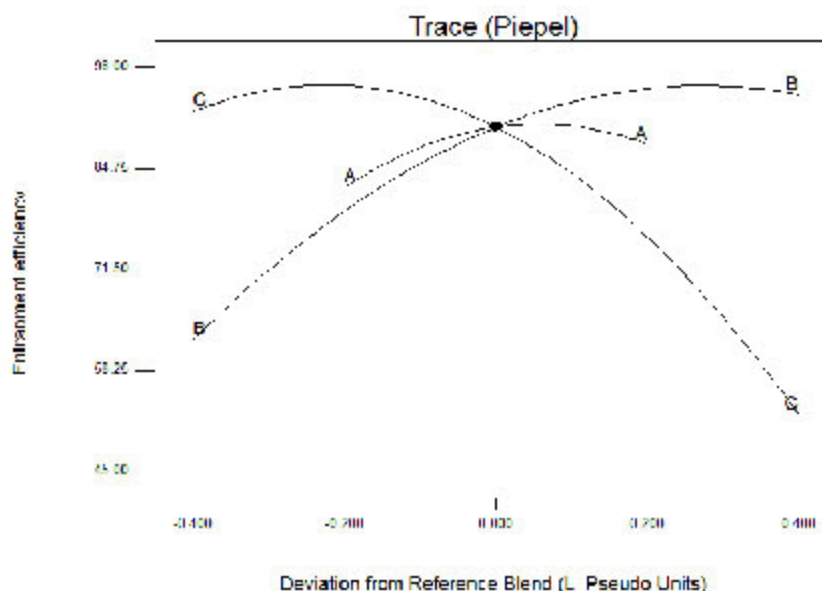


**Figure 5.8 Piepel's plot (A=HSPC, B=EggPC and C=Chol)**

Piepel's plot is a trace plot showing the effect of individual factors plotting the pseudo limits of one component keeping the ratio of the changeable amounts of the each components kept constant against the response. The responses are plotted as deviations from the reference blend i.e. centroid (pseudo center point of the constrained design). As it can be seen from the Figure 5.8, EggPC and HSPC is the factor with positive impact on Entrapment efficiency while cholesterol has negative effects.

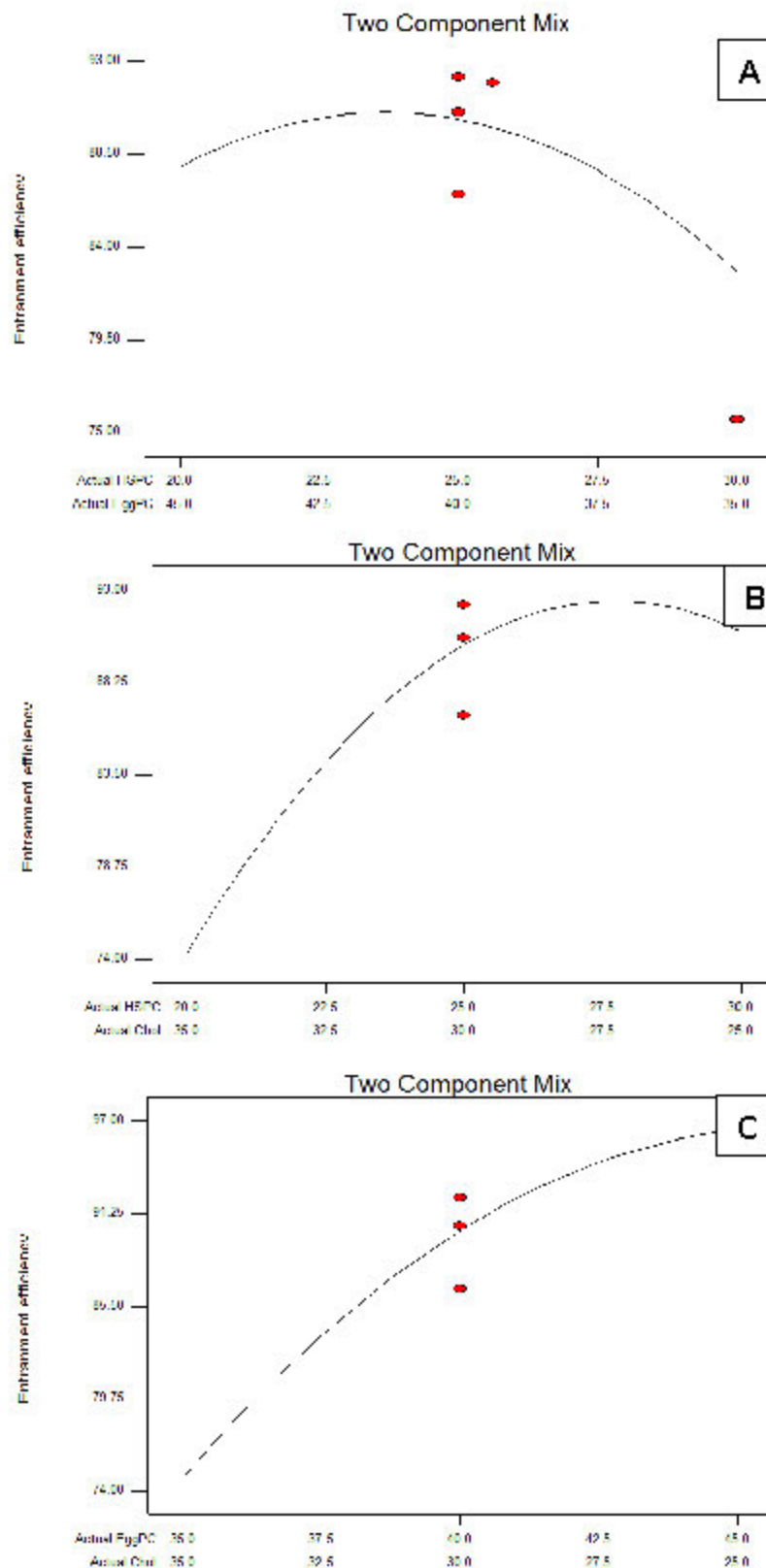


**Figure 5.9 Two-component mixture plots; A: effect of HSPC and EPC, B: effect of HSPC and Chol, C: effect of EPC and Chol**

Two component mix plots shows the combined effects of two components on the response keeping the value of another component constant at its centroid value. As it can be seen from the Figure 5.9, as the ratio of HSPC:EPC increases i.e. mole% of HSPC increases and mole% of EPC decreases, entrapment efficiency increases slightly and then decreases; however, the difference over the range is not significant. With the two component mix plots of HSPC and Chol and EggPC and Chol, similar trend of increase in entrapment efficiency was seen as the HSPC:Chol or EggPC:Chol ratio was increased. Cholesterol which due to its interdigitation capacity reduces the entrapment while HSPC and EggPC being a bilayer forming lipids provides hydrophobic bilayer which can accommodate more of PTX. Moreover, the EggPC which also has the unsaturated phospholipids in its components, allows more incorporation of DTX. This is apparently seen in the Figure that the EggPC has the highest effect on the entrapment efficiency of the PTX.

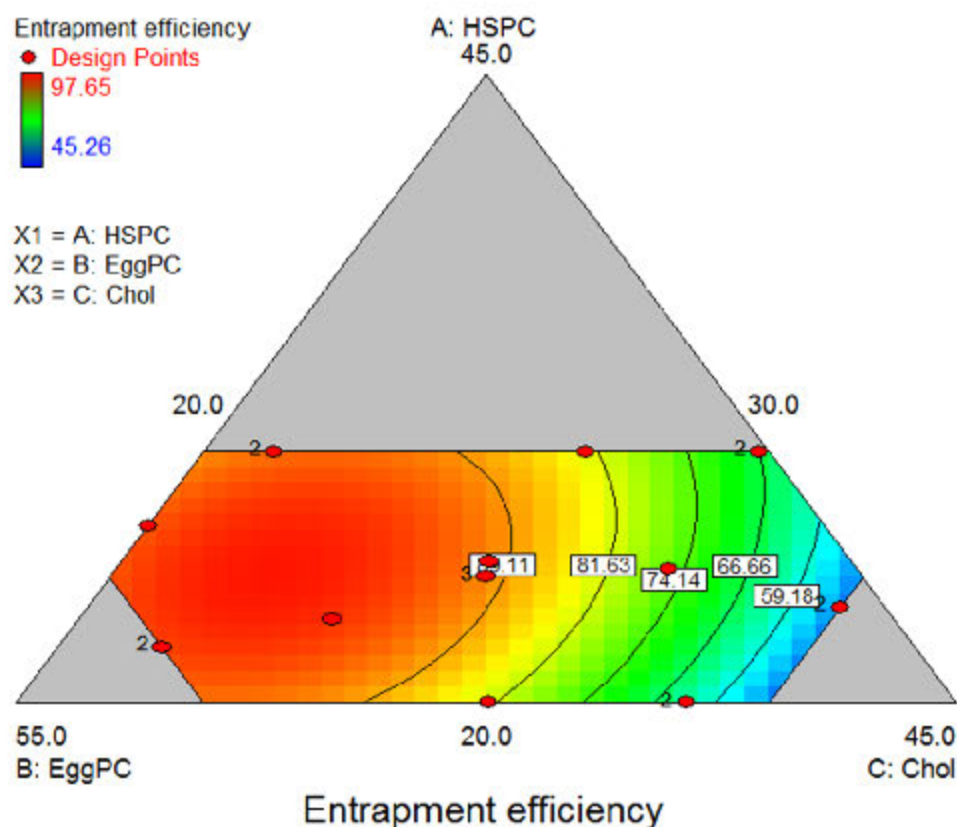
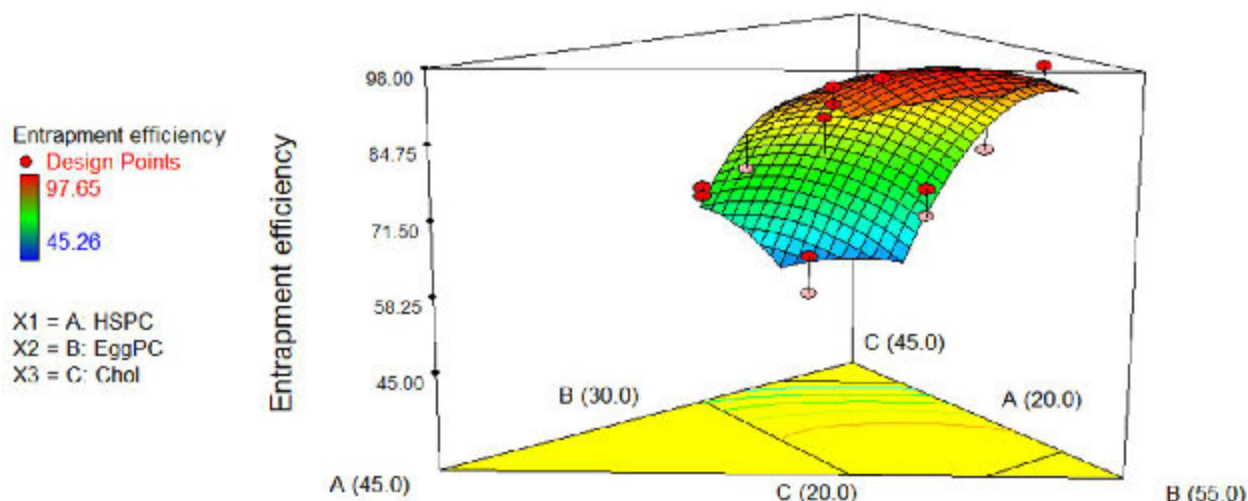


Figure 5.10 Contour plot of effects of different components on EE



**Figure 5.11 Response surface plot of effects of different components on EE**

Contour plot (Figure 5.10) and response surface plot (Figure 5.11) show effects of all three components on the entrapment efficiency. To summarize, with increasing mole% of EggPC and mole% of HSPC causes increase in the entrapment efficiency while increase in the Cholesterol level in the mixture brings about a decrease in the entrapment efficiency. The effects can be explained with similar justifications mentioned under the two component mix plots.

#### Equation for prediction of entrapment efficiency over design matrix

Equation for prediction of entrapment efficiency within the design matrix is given below.

Entrapment efficiency =

$$\begin{aligned}
 & -8.89033 && * \text{HSPC} \\
 & -1.80947 && * \text{EggPC} \\
 & -8.49164 && * \text{Chol} \\
 & +0.19468 && * \text{HSPC} * \text{EggPC} \\
 & +0.30303 && * \text{HSPC} * \text{Chol} \\
 & +0.18134 && * \text{EggPC} * \text{Chol}
 \end{aligned}$$

### iii. Selection of Formulation Parameters

Constraints applied to select the best formulation parameters based on the desired particle size and polydispersity index (Table 5.12).

**Table 5.12 Constraints Applied for Selection of Optimized Batch**

Name	Goal (to be optimized)	Lower Limit	Upper Limit
HSPC (mole%)	in range	20.0	30.0
EPC (mole%)	in range	30.0	50.0
Chol (mole%)	to maximize	20.0	40.0
Particle size (nm)	to minimize	101.4	286.5
Entrapment efficiency (%)	to maximize	45.26	97.65

All the affecting factors were to be optimized within the range chosen for design matrix except for the cholesterol level. Goal for cholesterol mole% was set to be maximized as the final liposomal formulation was to be used for the incorporation of the PTX-CD complex which requires higher cholesterol levels in the liposomes for their stability. Particle size was to be optimized at the minimum value possible in the range observed experimentally (104.4-286.5 nm) and entrapment efficiency was to be optimized at the minimum value possible in the experimentally observed range of 45.26% to 97.65%. Surface plots (Figure 5.12) show that the region with the lowest particle size doesn't coincide with the region with the lowest PDI which requires a trade-off between the selected parameters for selection of an optimized batch. The optimization was based on the desirability criteria which makes the best trade-off between the constraints and selecting a combination which satisfies the criteria the best for optimization and weighs the prediction based on a desirability index which ranges from 0 (for the least suited combination) to 1 (the best suited combination). The desirability plot which depicts the desirability index over the design is shown in Figure 5.13 showing a flag where the optimized batch lies.

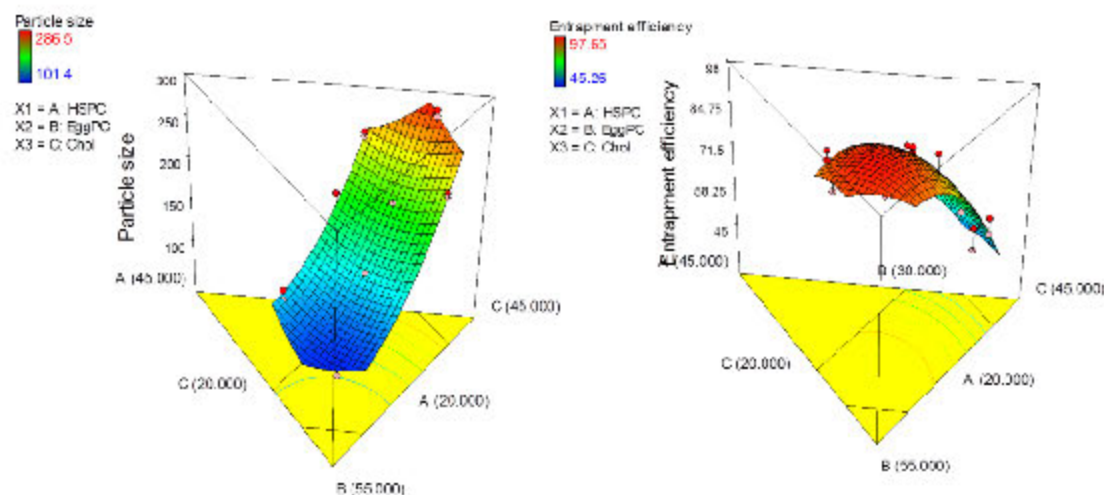


**Figure 5.12** Surface plots showing optimum particle size and %EE at best trade-off for the constraints

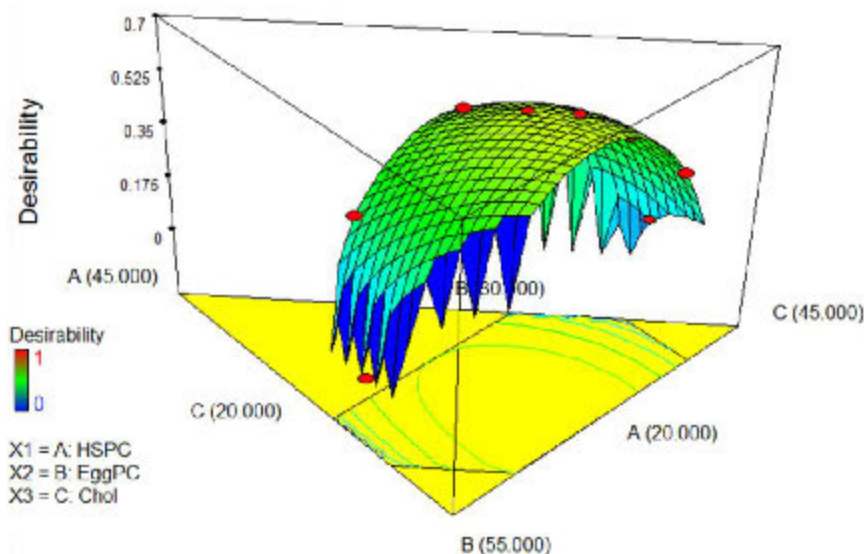


**Figure 5.13** Desirability Plot for Selection of Optimized Batch

Based on the maximum desirability, one formulation (desirability 0.690) was found to best fit the selection constraints. Predicted responses of this batch were 143.3 nm particle size and 89.97% entrapment efficiency (Table 5.13).

**Table 5.13** Optimized Batch Parameters Based on Desirability

HSPC	EPC	Chol	Particle Size	Entrapment efficiency	Desirability
22	43	30	143.3	89.97	0.690

**iv. Point Prediction and Confirmation:**

Table 5.14 below shows predicted response for the solution selected above along with the Standard deviation, 95 % confidence interval and 95% tolerance interval of the response. Confirmation of the response was done by carrying out the experiment using the selected factor values in triplicate. Table 5.15 shows and confirms that experimental and predicted values are in good agreement concluding the suitability of the selected model for optimization.

**Table 5.14 Predicted Responses of the Optimized Batch**

Response	Predicted	SEM	95% CI* low	95% CI high	95% TI# low	95% TI high
Particle Size (nm)	143.3	3.03	136.78	149.87	126.65	160.00
Entrapment Efficiency (%)	89.97	1.78	86.12	93.83	80.16	99.79

\* CI indicates Confidence Interval

# TI indicates Tolerance Interval (99% of the population will be within this range for all future batches)

**Table 5.15 Experimental Confirmation of the Predicted Responses**

Response	Predicted	SEM	Experiental Mean	Std Dev
Particle Size (nm)	143.3	3.03	149.6	4.6
Entrapment Efficiency (%)	89.97	1.78	92.6	1.98

\*Experiments were performed in triplicate.

**Optimization of process variables**

The process variables like hydration time, temperature and size reduction of the prepared liposomes were optimized for achieving maximum entrapment and minimum particle size. From the result obtained, 40 min hydration time was selected and hydration temperature of 55°C. At these selected conditions, extrusion cycles were optimized wherein the number of passes through 0.4 $\mu$  filter was optimized at 8 cycles. At the end of

successive passes through filter of decreasing size the size at end of pass through 0.4 $\mu$  filter was 289.6 $\pm$ 21.6 nm. Now, the particle size was determined after extrusion through 0.1 $\mu$  filter (Table 5.16). All the extrusion process was carried out at T<sub>g</sub> of liposomes.

**Table 5.16 Optimization of process variables**

Process Parameters		Entrapment efficiency (%)	Particle Size (z-average)
Hydration time	20 min	79.36 $\pm$ 3.68	1.26 $\mu$
	40 min	93.67 $\pm$ 2.96	1.34 $\mu$
	60 min	92.40 $\pm$ 3.01	1.19 $\mu$
Hydration temperature	50 $^{\circ}$ C	56.26 $\pm$ 5.94	1.49 $\mu$
	55 $^{\circ}$ C	92.69 $\pm$ 2.73	1.39 $\mu$
	60 $^{\circ}$ C	89.36 $\pm$ 4.69	1.36 $\mu$
Extrusion cycle	3 cycles	93.84 $\pm$ 3.21	201.8 $\pm$ 12.6 nm
	5 cycles	92.98 $\pm$ 4.36	154.5 $\pm$ 8.8 nm
	8 cycles	92.67 $\pm$ 4.87	129.8 $\pm$ 4.6 nm

#### 5.4.2 Preparation of PEGylated conventional liposomes

PEGylation of the conventional liposomes was carried out using varying amount of DSPE mPEG 2000 viz 1 mol%, 3 mol%, 5 mol% and 7 mol%. Effect of these varying concentration of PEGylated lipid after pre-insertion in lipid films on physico-chemical parameters of the formed liposomes was evaluated by measuring the particle size, zeta potential, % drug content and pH of the prepared formulation. The results are provided in Table 5.17. Increase in mol% of mPEG led to a slight increase in the % drug loading in liposomes. This may be due to increase in the area of the liposomal bilayer due to incorporation of larger lipid molecule in its structure. This can also be assumed from the increase in size of liposomes observed at increasing PEGylation levels. Further, there was a decrease in zeta potential for the liposomes due to the negative charge imparted by the phosphate group of DSPE mPEG 2000. Based on these results, the incorporation of 5 mol% of PEGylated lipid can be selected. A higher amount of PEGylation i.e. 7 mol% was also tested but compared to 5 mol% no improvement in the properties were observed

expect for significant increase in particle size. Also, a higher level of PEGylation may also interfere with the transfection efficiency of the prepared system and hence, 5 mol% of PEGylated lipid may be selected. Further, apart from these physico-chemical parameters, other studies that were carried out to optimize the PEGylation amount includes electrolyte induced flocculation and opsonization study.

**Table 5.17 Effect of PEGylation (\*significant increase in the particle size at PEGylation level of 3 mol% ( $p < 0.05$ ) and  $\geq 5$  mol% ( $p < 0.001$ ) compared to CLs.)**

<i>DSPE mPEG-2000 concentration</i>	<i>Particle size (nm) (<math>\bar{x}</math>- average)</i>	<i>Zeta potential (mV)</i>	<i>Entrapment efficiency %</i>	<i>pH</i>
Conventional liposomes (CLs)	120.9 $\pm$ 3.5	4.62 $\pm$ 0.18	90.59 $\pm$ 2.63	4.56 $\pm$ 0.04
PLs at 1 mol%	132.5 $\pm$ 4.2	1.10 $\pm$ 0.09	91.84 $\pm$ 1.96	4.62 $\pm$ 0.05
PLs at 3 mol%	141.6 $\pm$ 3.8*	-2.03 $\pm$ 0.12	92.26 $\pm$ 2.28	4.91 $\pm$ 0.08
PLs at 5 mol%	150.3 $\pm$ 3.2**	-3.2 $\pm$ 0.09	93.45 $\pm$ 2.20	5.33 $\pm$ 0.15
PLs at 7 mol%	198.8 $\pm$ 6.2**	-4.1 $\pm$ 0.11	93.01 $\pm$ 2.61	5.41 $\pm$ 0.09

PEGylated liposomes were also prepared by using HSPC and Egg PC alone along with the combination of lipids, to determine the effect of combination of phospholipids on the entrapment and particle size of the formed liposomes. It was observed that entrapment of PTX increased when combination of lipids was used rather than using a single lipid in preparation of PLs. Thus, use of combination of lipid would improve the entrapment of hydrophobic drugs in the bilayer. This may be due to the alteration in the rigidity of bilayer due to combination, which is difficult to achieve using a single lipid in the composition. However, the particle size for the liposomes varied considerably in case individual lipids were employed, with lowest in case of Egg PC (Table 5.18). Zeta potential of PLs formed from individual lipids was of the order of -1 to -4 which will only be due to the PEGylated lipid as other lipids are neutral in character.

**Table 5.18 Comparison of PEGylated liposomes prepared using individual and combination of lipid**

<i>Composition of PEGylated (5 mol%) liposomes</i>	<i>Entrapment efficiency %</i>	<i>Particle Size (z-average)</i>
HSPC and Egg PC	93.45 ± 2.20	150.3 ± 3.2
HSPC alone	84.81 ± 3.36	128.6 ± 3.6
Egg PC alone	78.67 ± 3.14	101.9 ± 2.2

### 5.4.3 Preparation of Double loaded PEGylated liposomes

On the basis of preliminary studies of interaction of PTX with various lipids and encapsulation efficiency of PTX, HSPC and Egg phosphatidylcholine were selected in combination with cholesterol to prepare liposomes. Liposomes were optimized to evaluate the effect of various process parameters (hydration time, hydration volume and temperature) and formulation parameters (total lipid content, drug to lipid ratio, internal lipid ratio) using D - optimal design. PTX being lipophilic shows high entrapment efficiency by incorporation in liposomal bilayer. The schematic representation of preparation method for DLPLs is provided in Figure 5.14. Despite high entrapment the amount of drug, loading efficiency of the liposomal system is low as it depends on drug:lipid ratio and offered space of lipid bilayer. Further, it has been reported that for drug entrapped in bilayer of liposomes gets leached readily due to permeability changes. This may lead to membrane destabilization and rapid release of drug in vivo. Herein, the lipid composition was first optimized for plain PTX loaded in bilayer to achieve maximum entrapment efficiency. The same composition was used for double loading of liposomes and it was observed that there was insignificant change in the physicochemical properties of the system due to incorporation of complex during the hydration stage. The highest amount of drug loading was observed at 1:30 drug: lipid molar ratio. Below this ratio, precipitation was observed. To provide long circulation time, both the liposomal systems were PEGylated using 5 mol% of DSPE-mPEG 2000 lipid. The PLs and DLPLs, with 5 mol% DSPE-PEG2000, showed very less flocculation in sodium sulfate solution as compared to 1 mol% and 3 mol% (see preceding section).

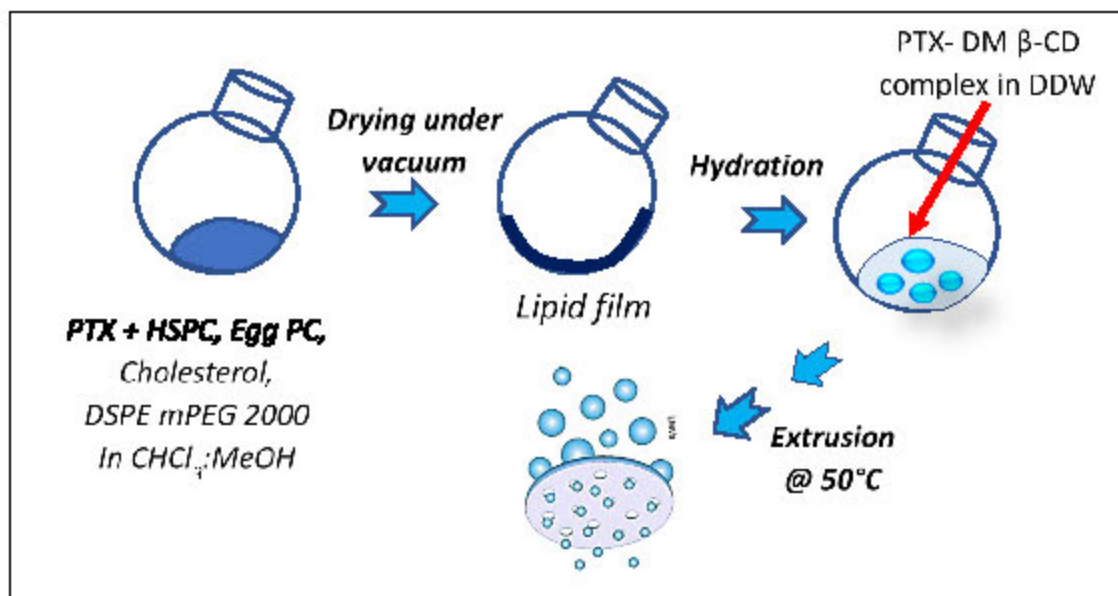


**Figure 5.14 Preparation of DLPLs**

Generally, preparation of liposomes encapsulating complexes are carried out giving preferentially selection to only high melting lipid; therefore, HSPC was used ( $T_c \sim 56^\circ\text{C}$ ) to impart rigid framework for maintaining stability of the liposomes in plasma and in vitro. However, cyclodextrin are known to affect bilayer stability dependent on degree of membrane fluidity and entrapped solute. Therefore, simultaneous incorporation of cholesterol along with use of lipid with high  $T_c$  was necessary to impart membrane robustness and flexibility. Results of the optimized batch indicated adequate physicochemical stability of the liposomal suspension during stability studies. The crystal-free liposome formulation with the highest amount of PTX incorporated in bilayer was 0.58 mg/ml. This result is in agreement with previous report wherein, PTX loading of 3-3.5 mole % (PTX to phospholipids) has been found to be stable for weeks to months. When, PTX and PTX-DM $\beta$ CD ICs were simultaneously loaded into the liposomal system. DLPLs could lower drug:lipid molar ratio from 1:30 for PLs to 1:16 which plays a significant impact in decreasing the total lipid content as well as increasing the drug load.

## 5.4.4 Characterization of PEGylated Conventional and double loaded liposomes

### 5.4.4.1 Particle size and Zeta Potential analysis

Size of the optimized PLs were of the order of  $150.3 \pm 3.2$  nm (Figure 5.15) with PDI of  $0.11 \pm 0.005$  and zeta potential of  $-3.2 \pm 0.09$  mV (Figure 5.16), whereas the DLPLs had size of  $162.8 \pm 4.1$  nm (Figure 5.17) with PDI of  $0.18 \pm 0.004$  and  $-5.6 \pm 0.14$  mV zeta potential (Figure 5.18). The results of DLS confirmed the nano-size of the formulation which is important for preventing opsonization of the liposomes by phagocytes and may also be implicated for enhanced efficacy of our system by its extravasation to the tumor sites through enhanced permeation and retention effect. The slight negative charge imparted to the liposomes may be due to the DSPE-mPEG chain bearing phosphate groups (68) (62).

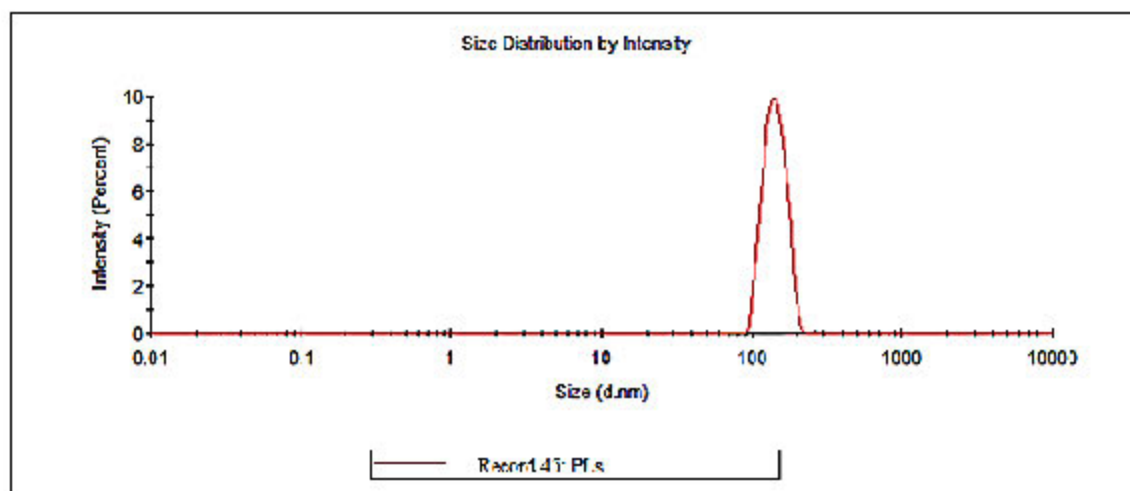


Figure 5.15 Particle size analysis for PLs

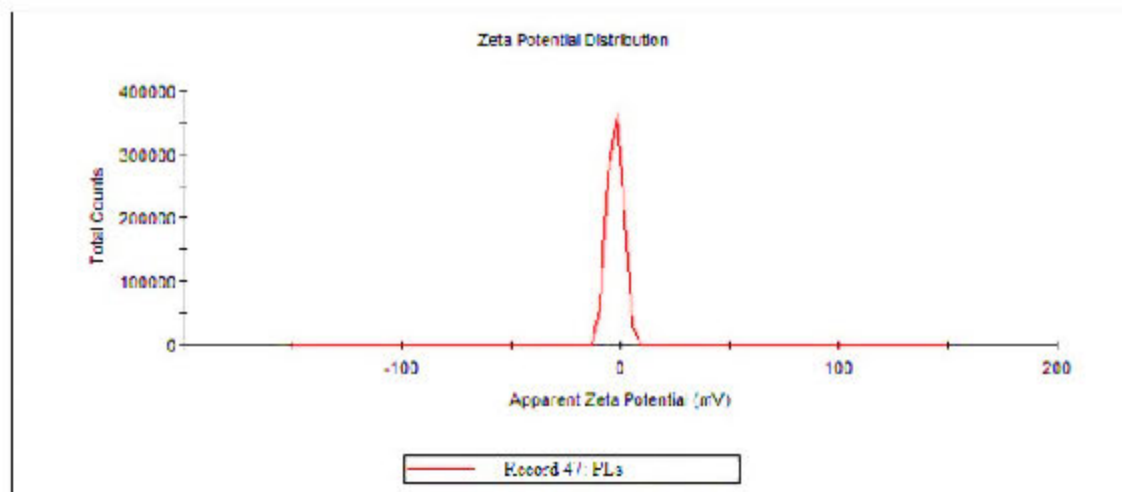


Figure 5.16 Zeta potential for PLs

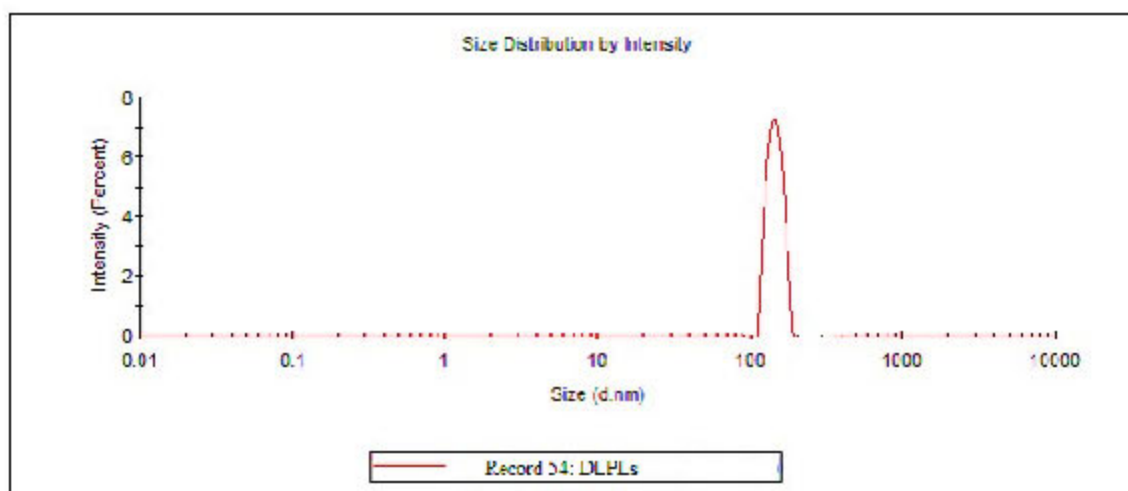
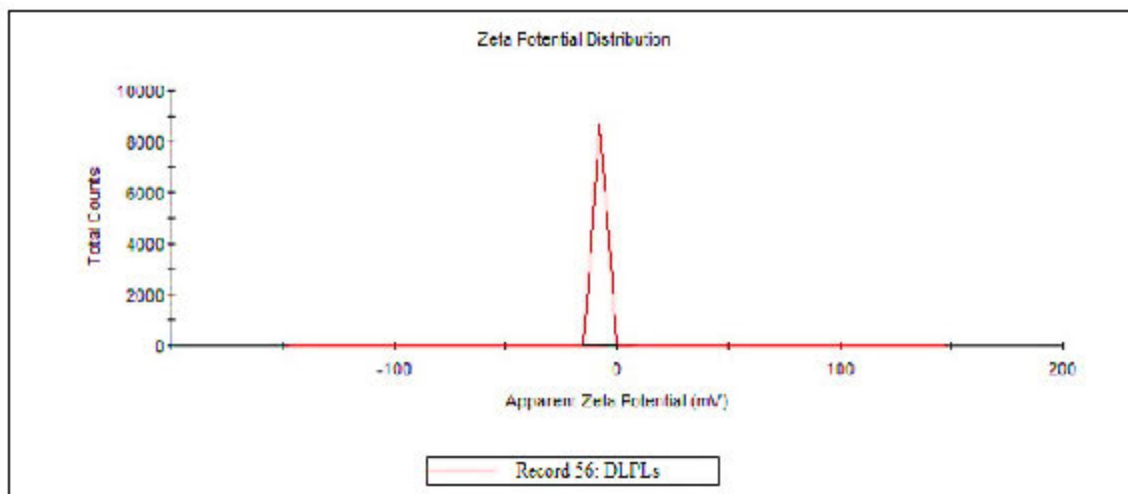


Figure 5.17 Particle size analysis for DLPLs



**Figure 5.18 Zeta potential for DLPLs**

#### 5.4.4.2 Cryo-TEM

TEM images of PLs and DLPLs showed particle size around 130 nm. Though this is in disagreement with that of particle size obtained by dynamic light scattering, such difference can be easily realized as DLS reports the hydrodynamic diameter of the particles whereas in TEM analysis the size obtained is of the particle fixed in grid. Cryo-TEM images (Figure 5.19) displayed a monodisperse liposomal sample having a unilamellar character and having spherical shape.

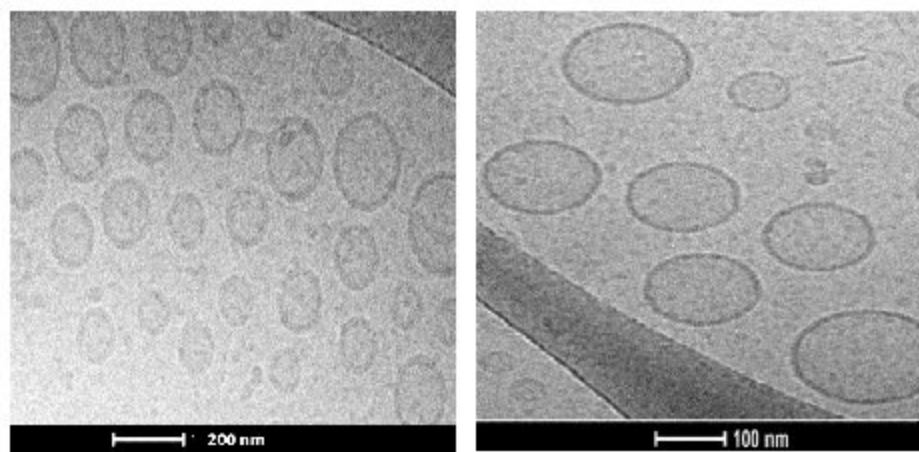


**Figure 5.19 Cryo-TEM image of PLs (left) and DLPLs (right).**

#### 5.4.4.3 Entrapment efficiency and drug loading

The entrapment efficiency for PTX alone loaded into phospholipid bilayer was determined as  $92.67 \pm 4.8\%$ . At drug to lipid ratio of 1:30, liposome containing 68  $\mu\text{moles}$  lipids was able to load 2.10  $\mu\text{moles}$  of PTX into bilayer. At the same time,  $30 \pm 2.7\%$  of PTX-DM $\beta$ CD could be entrapped into aqueous core. Thus, DLPLs could load 1.2 mg of PTX/ml in liposomes which is 2-fold the loading efficiency of PTX loaded conventional liposomes (0.58 mg PTX/ml) or double loaded liposomes containing 68  $\mu\text{moles}$  of lipid could load 4.21  $\mu\text{moles}$  of PTX. Drug loading of 5.8 mole % (PTX to lipid mole%) was achieved for DLPLs which was almost double the loading of PLs (3 mole%).

#### 5.4.4.4 In vitro drug release study

The *in-vitro* release study of PTX from Taxol®, PLs and DLPLs were carried out by dialysis method using PBS (pH 7.4) as release media to mimic the physiological condition, for 24 hr at 37 °C. The addition of 0.1% (v/v) tween-80 to the release medium was done to maintain sink condition. PTX release from Taxol® was rapid as  $92.17 \pm 5.3\%$  of drug was released within 24 hr in PBS pH 7.4 release medium. Both the liposomal system exhibited an initial burst release of 20% of its content at 2 hr that may be due drug incorporated in the bilayer of liposomes. However, at the end of 24 hr, PTX release from PLs and DLPLs was only  $39.56 \pm 3.1\%$  and  $28.39 \pm 2.6\%$  in PBS pH 7.4 release medium at 37 °C. It can also be noted that the DLPLs show a slower release compared to PLs, which may be due to two reasons. First may be the higher diffusional barrier encountered by complex to pass through the bilayer which may be the rate limiting step and other may be release of native PTX due to slow dissociation and equilibrium between the native and complex form of PTX in IC. Thus, the prepared liposomal system may be regarded to act as reservoir system for the encapsulated PTX molecules. While for Taxol® rapid and complete release (92%) of drug was observed at the end of 24 hr that may be due to the presence of solubilizers in its composition which present no barrier to the diffusion of drug to the release medium. The release profile of DLPLs and ILs did not exhibit any significant difference at any time point tested (Figure 5.20).

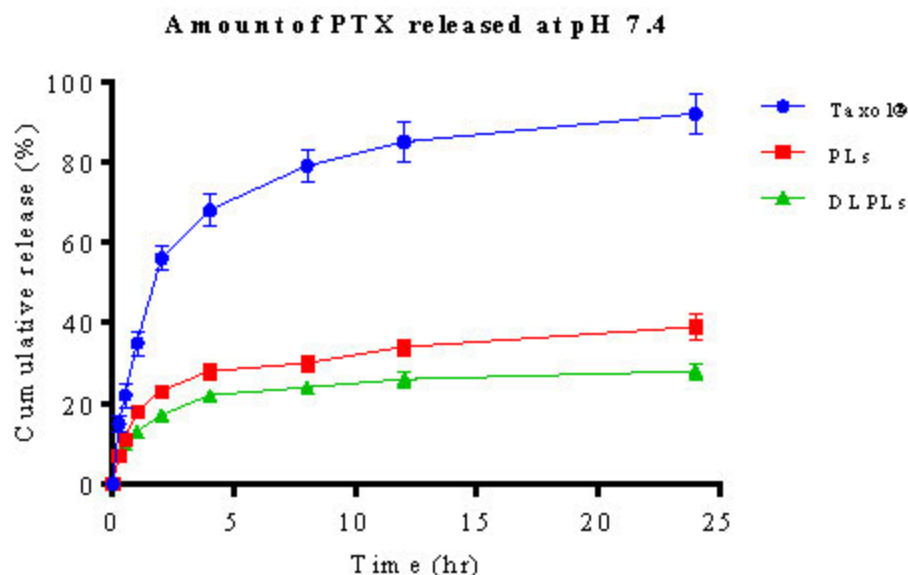


**Figure 5.20** In vitro release of PTX from Taxol®, PLs and DLPLs up to 24 hr at 37 °C in phosphate buffer saline at pH 7.4

#### 5.4.5 Additional characterization for PEGylated double loaded liposomes

##### 5.4.5.1 DSC and FTIR

Figure 5.21; Figure 5.22 and Figure 5.23 shows thermal analysis of PTX, physical mixture of drug with lipids and PEGylated liposomes – DLPLs (@ 5 mol%) respectively using DSC technique. PTX exhibit sharp endothermic peak at around 216-218°C which shows its characteristic melting point. That peak was absent in DSC spectrum of PEGylated liposomes confirming the complete encapsulation and amorphization of PTX in the bilayer along with successful retention in the aqueous core. The analysis was performed at high heating rates to detect the presence of even small amount of drug that may have gone polymorphic changes. The physical mixture exhibits additional peaks at temperature <100°C which may be due to the lipid component in the mixture.

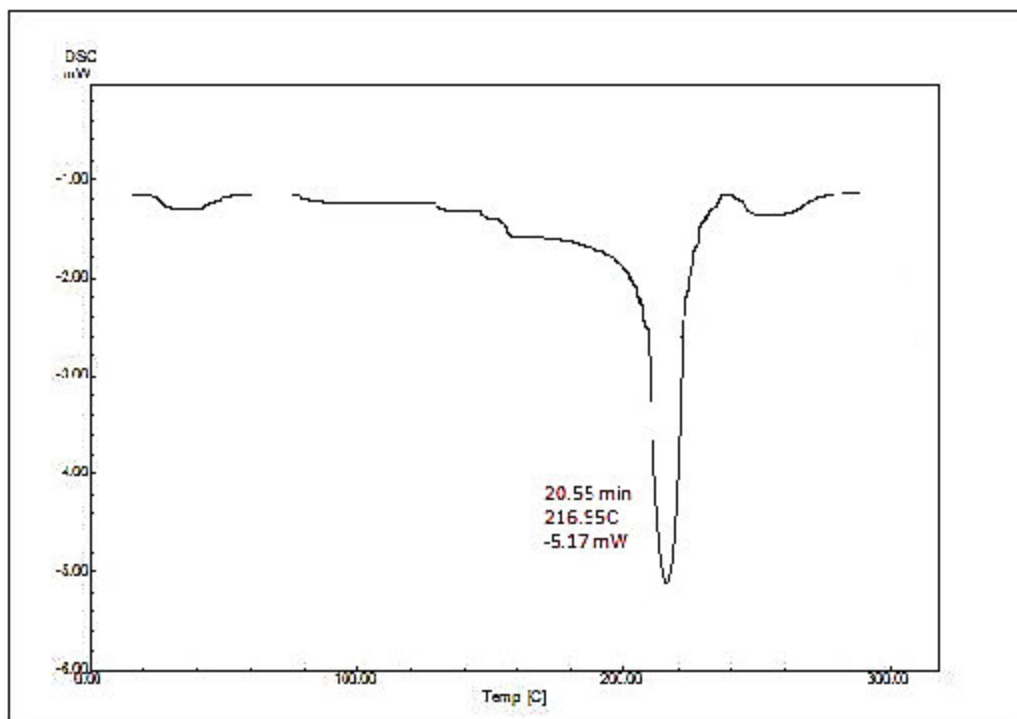


Figure 5.21 DSC thermogram of Paclitaxel

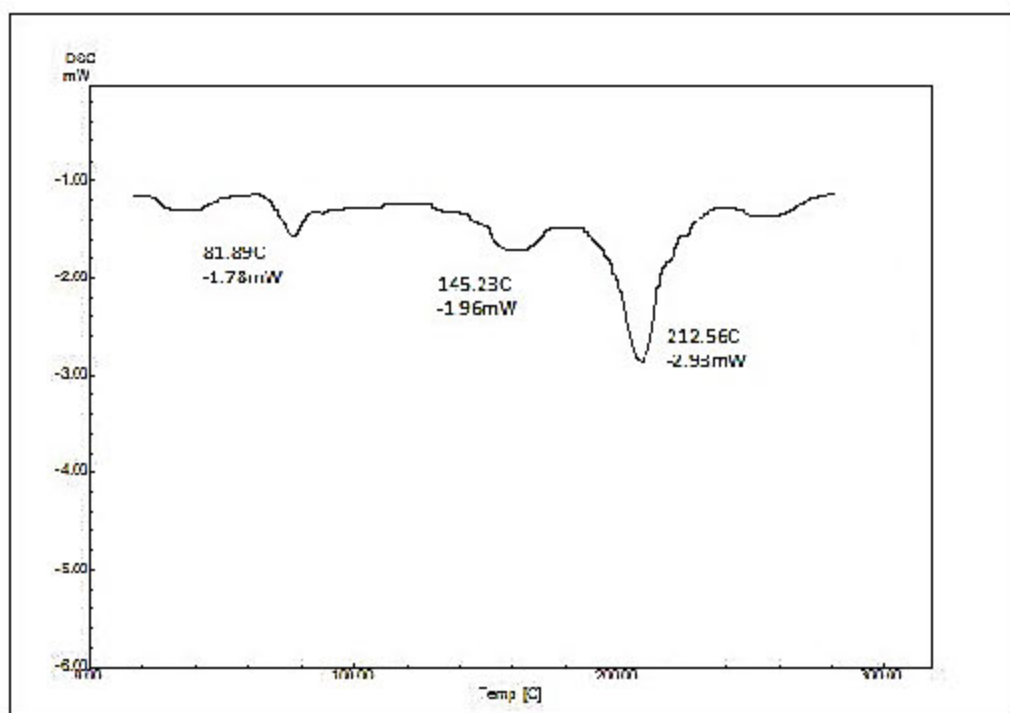
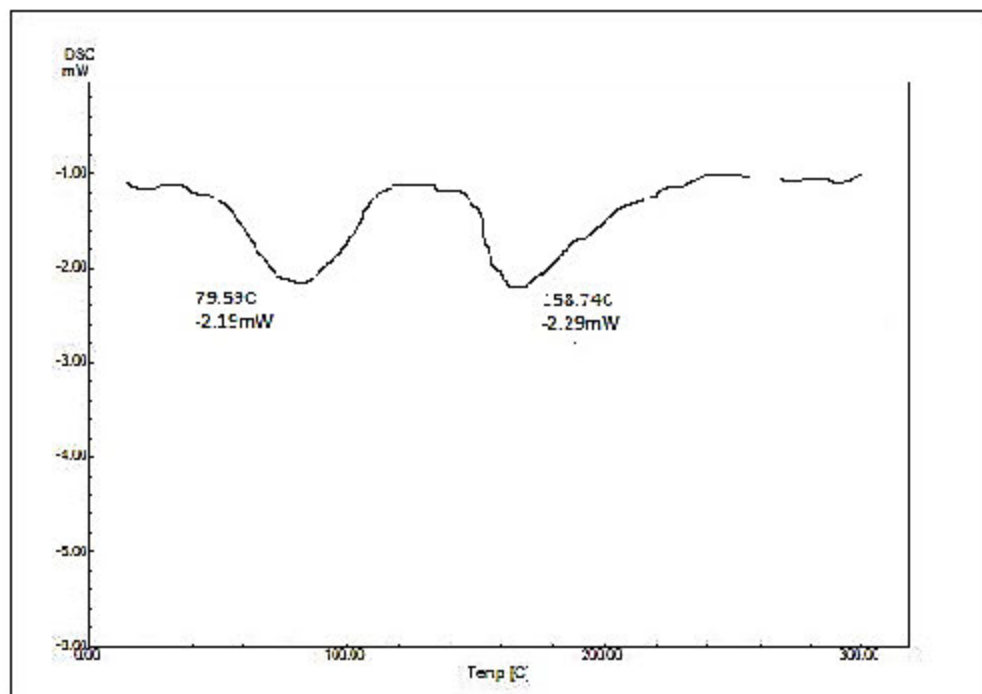


Figure 5.22 DSC thermogram of physical mixture of drug with lipids



**Figure 5.23 DSC thermogram of DLPLs**

Figure 5.24, Figure 5.25 and Figure 5.26 shows the FTIR spectra of PTX, Physical mixture and DLPLs respectively. Spectra of PTX drug pellets exhibit strong absorption bands in the range of  $1730\text{ cm}^{-1}$ – $1600\text{ cm}^{-1}$ ,  $1380\text{ cm}^{-1}$ – $1180\text{ cm}^{-1}$  and  $900\text{ cm}^{-1}$ – $710\text{ cm}^{-1}$ . These characteristic peaks are retained in the physical mixture of drug with lipids with a broadening effect and a decrease in intensity of principal peaks at  $1730\text{ cm}^{-1}$  and  $1300\text{ cm}^{-1}$ . Whereas, in case of DLPLs, all characteristic pertaining to PTX are absent, indicating the complete encapsulation of drug in the bilayer and only a diffused peaks throughout the spectra at wavenumber higher than  $1400\text{ cm}^{-1}$  are observed.

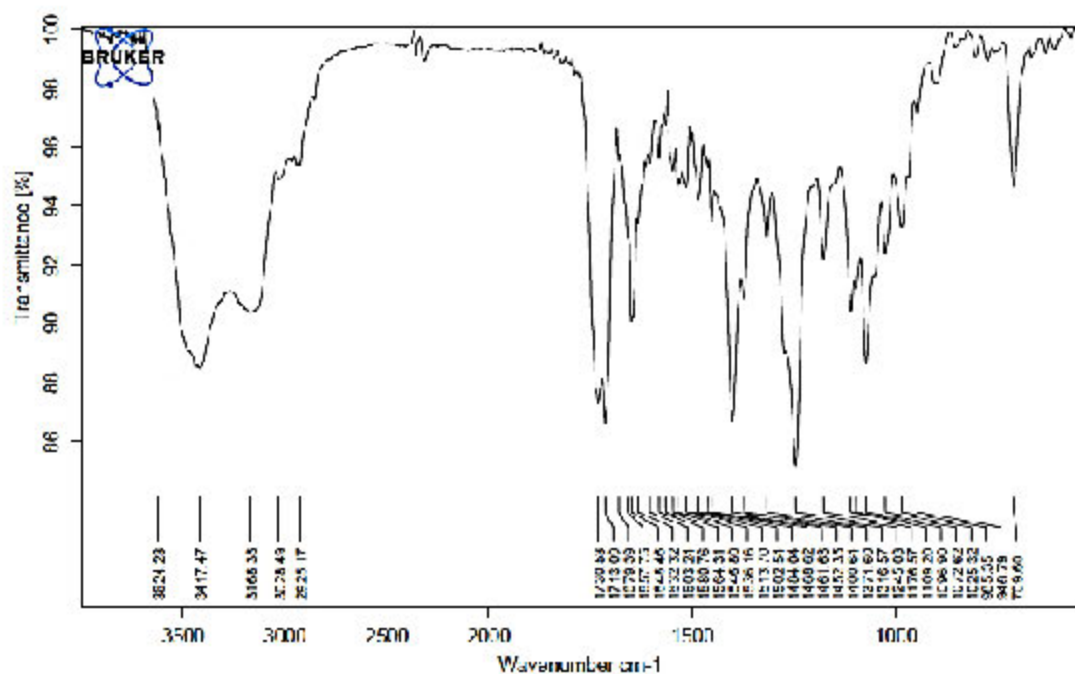


Figure 5.24 FTIR spectra of Paclitaxel

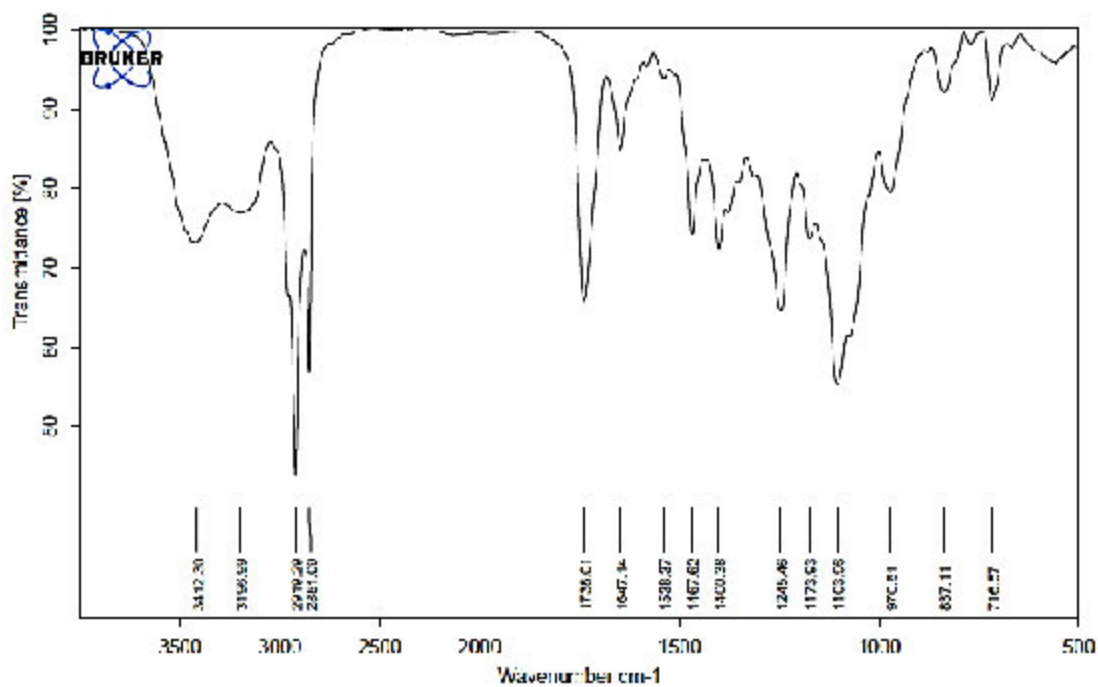


Figure 5.25 FTIR of physical mixture of drug with lipids

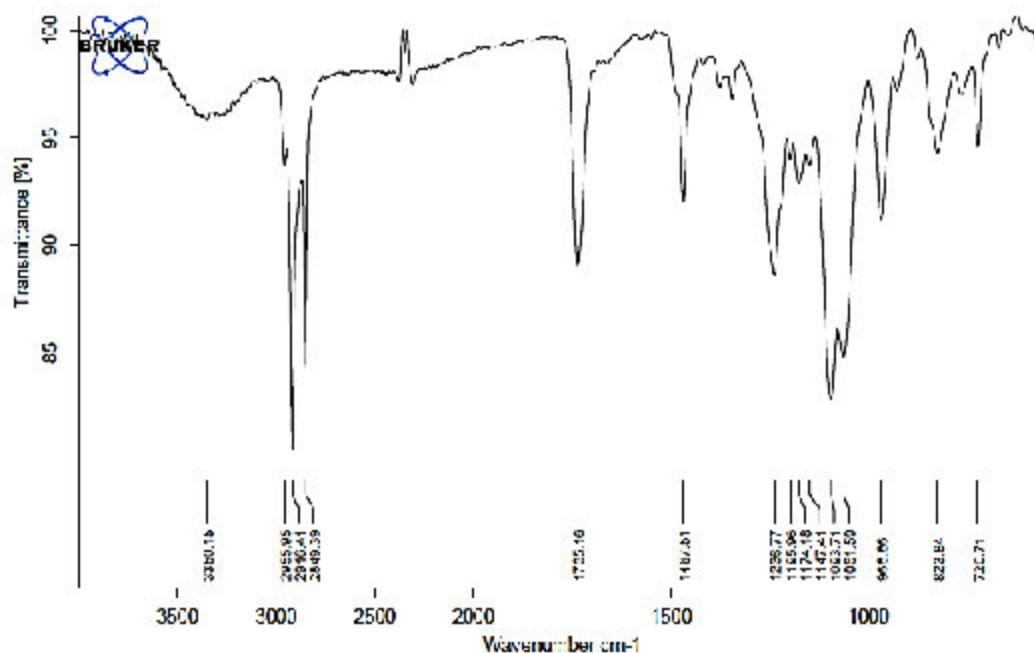


Figure 5.26 FTIR of PEGylated liposomes (DLPLs)

#### 5.4.5.2 Olympus microscopy:

The optical microscopic image of the DLPLs before and after extrusion through membrane filter at 20x magnification are presented in the figure 5.27 which confirms the reduction in size and spherical shape of liposomes with multivesicular structure. Figure also present the crystals of PTX in the liposomal suspension that were typically observed when the formulation were not optimized.

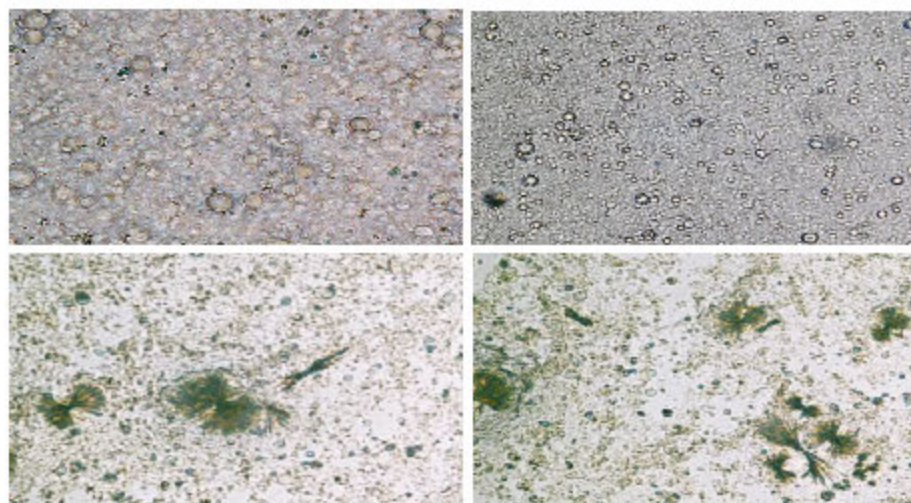


Figure 5.27 Optical microscopy image of DLPLs before and after extrusion (above) and Drug crystal (below) at 20X

### 5.4.5.3 Sodium Sulphate induced flocculation

Presence of electrostatic double layer barrier around the particles prevents the particle from aggregating, a phenomenon responsible for imparting stability to the colloidal systems. Competitive forces of repulsion and attraction are responsible for determining the stability of a colloidal system. Herein, for PEGylated liposomes, there is existence of a hydrated barrier of mPEG chain on the surface of liposomes, whose stability is evaluated by salt induced flocculation. The ionic imbalance induced by presence of electrolyte in the media will lead to failure of electric double layer and will result in aggregation of the liposomes leading to increase in the optical density of the system. However, presence of PEG will provide a steric barrier to the nanoparticle system to a greater extent even after the electric double layer gets destroyed.

The results of salt induced flocculation for CLs and DLPLs are presented in the table and figure below. As evident from the results, the CLs that do not have PEG chain extending from their structure began to destabilize i.e. showed aggregation or increase in optical density of the system was observed, even by incubating them with 0.2 M  $\text{Na}_2\text{SO}_4$ . An increase in turbidity of the system was observed as the concentration increased to 1.0 M. However, in case of liposomal system being PEGylated by varying amount of DSPE mPEG 2000 lipid, all showed comparative less tendency to aggregate/ flocculate and higher stability. From among the 4 levels screened, the concentration of PEGylated lipid at which minimum flocculation was observed was 5 mol%. To assess the impact of electrolytes on physical stability, particle size of the liposomes was also measured at each electrolyte concentration. It was found that the particle size of CLs offered minimum resistance to aggregation and a drastic increase was observed after addition of successive concentration of electrolytes from 0.2 M to 1.0 M (Table 5.19). This may be due to the absence of any steric barrier for inducing flocculation of the liposomes in presence of ionic species. Whereas, PEGylation of DLPLs started to confer steric stabilization to the liposomes to some extent right from incorporation of 1 mol% of PEGylated lipid as evident from the less drastic increase in size of DLPLs compared to CLs. However, the size range of DLPLs increased above 200 nm just at 0.4 M concentration of electrolyte which denotes to the fact that the level is insufficient to maintain liposomal stability. At

PEGylation level of 5 mol% and above the DLPLs provided sufficient steric stabilization as evident from the threshold electrolyte concentration of 0.8 M at which the particle is less than 200 nm (Table 5.20). The effect of electrolyte on zeta potential values was found similar in all cases i.e. all approached neutral to slight positive values at 0.4M levels and remained more or less constant at all other concentrations.

Table 5.19 Impact of electrolyte on optical clarity of liposomes

<i>Sodium sulphate concentration</i>	<i>Absorbance value</i>				
	<i>CLs</i>	<i>DLPLs</i>			
		1 mol%	3 mol%	5 mol%	7 mol%
Distilled water	0.051	0.046	0.052	0.058	0.071
0.2 M	0.275	0.142	0.132	0.099	0.102
0.4 M	0.684	0.310	0.256	0.124	0.131
0.6 M	0.845	0.521	0.441	0.149	0.146
0.8 M	1.064	0.968	0.789	0.187	0.179
1 M	1.115	1.098	0.896	0.219	0.222

*Values are reported as mean±SD, n=3.*

Table 5.20 Effect of electrolyte on Particle size of liposomes

<i>Sodium sulphate concentration</i>	<i>Particle Size (nm)</i>				
	<i>CLs*</i>	<i>DLPLs</i>			
		1 mol%	3 mol%	5 mol%	7 mol%
Distilled water	109.6	134.6	141.1	162.8	164.9
0.2 M	359.2	286.2	256.6	165.1	168.1
0.4 M	994.1	569.5	342.2	172.6	170.9
0.6 M	1462.9	925.6	652.4	186.2	190.6
0.8 M	-*	1019.3	743.9	194.8	198.6
1 M	-*	-*	899.6	251.9	259.9

*Values are reported as mean±SD, n=3. \*\* Particle size >1.5µ*

*\*Mean particle size increased significantly (p<0.001) compared to DLPLs*

#### 5.4.5.4 In vitro serum protein adsorption study/opsonization study

Of the main mechanism leading to the failure of therapeutic efficacy of drugs administered by intravenous route as liposomal formulation is their rapid binding to the variety of proteins present in the human plasma and subsequent recognition and clearance via phagocytosis. Presence of polyethylene glycol chain on the surface of liposomes is hypothesized to confer a shell of hydration around the particles, thus leading to impairment of recognition and subsequent opsonization, making them undetectable by the phagocytosis clearance mechanism. This in effect confers long circulation characteristic to the formulation. It is thus important that the formulated system have this important characteristic of bypassing the clearance mechanism. It has been investigated that a direct relation exists between the amount of plasma protein bound to the liposomes and clearance rate. Thus, clearance of liposomes from the circulation *in-vivo* is largely affected by the amount of protein associated with the liposomes. As it is not feasible to determine the liposomes associated with the plasma proteins *in-vivo*, due to the rapid distribution across systemic circulation, a reliable method is to determine the amount of protein that gets associated with liposomes by *in-vitro* assay. These assays provide for easy estimation of the amount of liposomes associated with the proteins due to their recovery and thus can be useful for predicting the clearance behavior of the formulation. Thus, in present study, CLs and DLPLs were incubated with fetal bovine serum in a shaker incubator at 37°C for 1 hour. The percent recovery of the liposomes after incubation and separation through sepharose gel column was determined and are reported in Table 5.21.

**Table 5.21 % Liposomes Recovery**

<i>Formulation</i>	<i>Total lipid amount in liposomes (mg)</i>	<i>Amount of lipids recovered after incubation (3 ml) (mg)</i>	<i>% Liposome recovery</i>
CLs	42.2	25.13 ± 1.2	59.56 ± 4.6
DLPLs – 1 mol%	46.2	30.94 ± 1.6	66.98 ± 4.4
DLPLs – 3 mol%	48.9	34.92 ± 1.1	71.41 ± 5.6
DLPLs – 5 mol%	51.6	42.12 ± 2.0	81.63 ± 4.6

DLPLs – 7 mol%	54.3	45.91 ± 1.6	84.55 ± 5.4
----------------	------	-------------	-------------

As observed, the highest recovery was obtained with higher level of PEGylation of liposomes, which may be due to lesser association of the serum proteins with the liposomal fraction and enhanced steric stabilization imparted by the PEG chains extending from the liposomes, preventing association of serum components with the liposomes.

The recovered liposomes after incubation with serum were also analyzed for particle size and zeta potential and the results are present in Table 5.22. The highest increase in the size of the liposomes was observed in case of CLs which is obviously due to the higher association of serum proteins with liposomal surface in absence of any steric hindrance along with corresponding increase in zeta potential value to more negative side which may be due to the charge imparted by the serum proteins itself to the liposomes after incubation. In case of PEGylated liposomes, as the extent of PEGylation was increased there was a lesser increase in the size and zeta potential after incubation indicating lesser interaction between the components of the mixture during incubation. The systems with 5 mol% and 7 mol% displayed a non-significant increase in size which displays their favorable characteristic upon in-vivo administration.

**Table 5.22 Particle size and Zeta potential of liposomes before and after incubation with FBS**

<i>Formulation</i>	<i>Before incubation with serum</i>		<i>After incubation and separation</i>	
	<i>Size (nm)</i>	<i>Zeta potential (mV)</i>	<i>Size (nm)</i>	<i>Zeta Potential (mV)</i>
CLs	109.6 ± 1.4	-1.2 ± 0.2	144.9 ± 4.2	-30.1 ± 1.2
DLPLs – 1 mol%	134.6 ± 1.9	-2.2 ± 0.3	146.2 ± 5.1	-25.6 ± 1.5
DLPLs – 3 mol%	141.1 ± 2.2	-2.8 ± 0.1	151.5 ± 6.2	-17.2 ± 0.9
DLPLs – 5 mol%	162.8 ± 2.6	-5.4 ± 0.3	168.3 ± 3.0	-10.7 ± 0.8
DLPLs – 7 mol%	164.9 ± 2.1	-6.1 ± 0.3	173.4 ± 3.5	-9.5 ± 0.9

To further quantitate the amount of serum protein associated with the liposomes after incubation, BCA protein estimation method was used and the results are reported in table 5.23. After delipidating the extracted liposomes associated protein and assaying the amount of proteins by assay method as indicated, the highest level of protein binding was displayed by CLs and least by 5 mol% and 7 mol% of PEGylation. Therefore, concluding the above findings it can be stated that the DLPLs with 5 mol% of PEGylation will impart *in-vivo* higher circulation time and reduced protein binding in serum that are essential for their efficacy.

**Table 5.23 Amount of serum proteins associated with liposomes**

<i>Formulations</i>	<i>Amount of serum proteins (<math>\mu\text{g}</math>)</i>	<i>Lipids recovered in liposomes (<math>\mu\text{M}</math>)</i>	<i>Protein binding index <math>P_B</math>: <math>\mu\text{g}/\mu\text{M}</math></i>
CLs	382.62 $\pm$ 25.91	0.843 $\pm$ 0.049	453.46 $\pm$ 25
DLPLs – 1 mol%	236.89 $\pm$ 21.68	0.702 $\pm$ 0.032	336.59 $\pm$ 39
DLPLs – 3 mol%	219.63 $\pm$ 12.67	0.737 $\pm$ 0.068	297.36 $\pm$ 23
DLPLs – 5 mol%	203.15 $\pm$ 14.82	0.860 $\pm$ 0.045	236.78 $\pm$ 21
DLPLs – 7 mol%	210.78 $\pm$ 15.63	0.990 $\pm$ 0.031	212.54 $\pm$ 26

#### 5.4.5.5 Liposome membrane integrity test

For liposome membrane integrity test, incorporation of CF in high amount in liposomes was carried out at its quenching concentration. Thus, the fluorescence measured at any time point will be due to the leakage of CF from the lipid vesicles and its dilution in the release media. The latency of the liposomes reported in percentage after incubation with the serum was measured after separation of liposomes using Sephadex G-50 column chromatography. From the values of the Table 5.24, it can be inferred that the impact of presence of drug in form of complex or the presence of cyclodextrin is a prominent factor in determining the membrane stabilization effect as evidenced from the low initial % CF latency for DLPL compared of PLs. However, the addition of cholesterol in the lipid composition showed higher membrane integrity for the encapsulated load and the initial CF latency increased to 81%. Further, as evidence from release of CF, it can be inferred that incorporation of cholesterol for imparting membrane

fluidity had only marginal effect on the release of CF and thus will not affect release (Table 5.25).

**Table 5.24 Initial % CF latency of liposomes with PTX after incubation with serum at 37°C.**

<i>Composition</i>	<i>Initial % CF latency in fetal bovine serum *</i>
<i>HSPC Chol</i>	92 ±2.2
<i>PLs containing drug in bilayer</i>	90±2
<i>DLPLs containing drug without cholesterol in lipid composition</i>	68 ±1.5
<i>DLPLs containing drug</i>	81±1.8

\* Values are reported for experiment in triplicate (mean±SD)

**Table 5.25 % retention of encapsulated CF after incubation with serum proteins at 37°C**

<b>Liposomal Composition</b>	<b>CF retention (%) (mean±S.D) *</b>				
	<b>Incubation time (hr)</b>				
	1	2	3	6	24
<b>DLPLs without cholesterol</b>	93±1.6	88±1.4	84±2.1	81±1.9	78±1.6
<b>DLPLs</b>	96±0.9	92±0.6	89±1.1	85±0.8	81±0.9

\* Values are reported for experiment in triplicate (mean±SD)

A prominent advantage of use of modified CD such as DMβCD is the more lipophilic character of its core leading to better encapsulation of lipophilic molecules, and further having higher aqueous solubility availing benefits of using higher solution concentration for attaining higher encapsulation efficiency of the encapsulate. But, this advantage of bearing core having high lipophilicity also presents a formidable challenge of maintenance of membrane integrity during preparation of the liposomes. Free CD molecules extract lipids from the membrane during preparation causing its destabilization and reorganization. This reorganization of the components of liposomal membrane leads to leaching of free drug to the exterior compartment resulting in its initial rapid release in

the plasma or serum or the release media. Our result suggests that cholesterol has some positive impact in stabilization of the bilayer during preparation as evident from the high CF latency observed as compared to the DLPLs without cholesterol in lipid composition. This may be due to the fact that the amount of drug CD complex contains low amount of free CD available for leaching of membrane lipids.

#### **5.4.7 Lyophilization of PLs and DLPLs**

Both the liposomal formulations of PTX i.e. PLs and DLPLs were lyophilized to provide stability to the liposomes as storage in liquid state may present the chance of aggregation of liposomes leading to increase in particle size and/or may lead to leaching of drug from the liposomes thus impacting the drug content. Thus, in solid state the particle interaction arising due to molecular motion gets nullified and further the dry state of the formulation with minimal moisture content will remain stable during long period of storage.

Freeze drying of the system in solid state will decrease the physical stress on the system that are levied on the product during handling and transport leading to agitation and freeze thawing of the product thus affecting the stability of liposomes in liquid state (69). Further, lyophilized formulations are reported to have improved stability even on storage at room temperature and at accelerated storage condition (70, 71). But, an important factor to consider is that if the lyophilization cycle is not designed properly the surface of the liposomes may get damaged or there may be aggregation of the liposomes or difficulty in redispersion of the lyophilized cake may be observed. Surface damage may be due to crystallization of ice on the surface due to increase in local concentration of the liposomes leading to aggregation (71-74) (75).

Another important aspect is the selection of cryoprotectant. In our case, based on prior experience sucrose was selected (76, 77). It has been postulated that at specific concentration of sucrose, the particle motion is significantly suppressed during unfrozen state of lyophilization thus rendering the particle to be freeze drying without aggregating (71, 74).

To evaluate the effectiveness of sucrose bulking agent and as cryoprotectant, sucrose was used at four different concentrations (i.e. 5 %w/v, 10% w/v, 20% w/v and 25% w/v). Important consideration was given to select such a concentration wherein the resulting lyophilized cake has high bulk volume and prevent the integrity of the liposomes in the cake with minimal effect on particle size or in other words prevent fusion of the liposomes and/or maintain the morphology of the liposomes that may get invariably affected due to crystallization of ice on the surface. Both the liposomal system were freeze dried at same condition as the only difference between the two system was of the encapsulated material in the core and it was previously demonstrated that the two system does not differ much in physicochemical properties.

Results of the optimization of cryoprotectant are summarized in Table 5.26. As can be deduced from the result of particle size and PDI, a concentration of 20% sucrose was found optimum to minimally impact these parameters and obtaining a porous cake with ease of reconstitution. At lower concentration of 5% and 10%, the cakes obtained had collapsed thus indicating that these amounts are insufficient as cryoprotectant during lyophilization. Further, at 20% concentration, the reconstitution time, which gives idea about the time taken by formulation to return to its original dispersed state, for both the formulation was approximately 2 minutes (Table 5.27). At higher concentration of sucrose i.e. at 30%, also the characteristic of the liposomes was found consistent in terms of particle size and drug content. The moisture content in the lyophilized cake for both the formulation, an indicator of the effectiveness of the lyophilization condition chosen, was found to be < 3% w/w and indicates a higher stability on storage due to low moisture content.

Lyophilization process consist of important steps of freezing the formulation at low temperature followed by removal of water by sublimation at reduced pressure. As freezing step may cause increase in particle size due to fusion and which in effect may affect the polydispersity of the liposomes along with challenge in the membrane integrity of the liposomes, we have evaluated changes in particle size, PDI and drug content for the lyophilized formulation. Result indicate only marginal increase in average particle size for both the liposomal system, a slight rightward shift in the PDI indicating minimal fusion and retention of the drug content indicating integrity of the system. Thus, both the

PLs and DLPLs exhibited sufficient initial stability at the optimized level of cryoprotectant and lyophilization cycle designed (based on prior experience).

**Table 5.26 Effect of lyophilization on particle size and zeta potential of PLs and DLPLs**

Lipoplexes	Sucrose concentration (%w/v)	Particle Size* (nm)	PDI* (Polydispersity index)	Drug content (%)	Zeta Potential (mV)
PLs	Before lyophilization	150.60±4.52	0.115±0.009	96.23±0.8	-3.5± 0.6
	5%	459.36±20.6	0.425±0.098	92.24±1.1	14.5±2.2
	10%	256.5±18.5	0.359±0.072	94.45±1.5	21.3± 3.5
	20%	156.2±10.2	0.160±0.018	95.54±1.0	29.4±4.8
	30%	155.6±8.4	0.142±0.023	95.87±0.9	31.9±4.9
DLPLs	Before lyophilization	165.6±8.8	0.185±0.013	97.63±0.8	-5.9± 0.8
	5%	376.6±39.1	0.412±0.068	89.54±2.4	18.5±4.1
	10%	225.5±26.5	0.299±0.046	93.61±0.9	26.2±3.6
	20%	171.8±11.9	0.206±0.010	96.14±1.8	36.9±4.8
	30%	169.4±14.6	0.201±0.015	96.30±1.2	35.9±4.5

*\*Experiments were performed in triplicate.*

**Table 5.27 Reconstitution time and water content of lyophilized liposomes**

Liposomes	Reconstitution time	Water Content (%w/w)
PLs	2 min	2.09±0.21
DLPLs	2 min	2.45±0.35

*\*Experiments were performed in triplicate.*

#### 5.4.8 Stability studies

In order to produce a commercially viable drug product the liposomes must exhibit physical stability (78). For a pharmaceutically acceptable liposomal product the preferred stability period for the formulation may range up to 1 to 2 years when stored at either room temperature or at refrigerated condition. In order to meet this requirement of extended period of storage, lyophilization becomes a prime resort for stabilizing the liposomal product. However, simply lyophilizing the formulation cannot ensure its

stability for the shelf life as its physicochemical properties may change and hence monitoring the real-time stability is important. To evaluate the stability of formulations, particle size, zeta potential and % drug content was determined.

The chemical stability data indicated a 15% and 10% drop in assay at  $25 \pm 2^\circ\text{C}$  and  $2-8^\circ\text{C}$  respectively upon liquid state storage of formulation. However, there was insignificant change ( $p > 0.05$ ) in assay upon lyophilized state storage at both  $25 \pm 2^\circ\text{C}$  and  $2-8^\circ\text{C}$  conditions. The data of physical stability showed acceptable results for description at both conditions. In addition, particle size showed an increasing trend in  $25 \pm 2^\circ\text{C}$  and  $2-8^\circ\text{C}$  conditions for liquid state. While, there was insignificant change ( $p > 0.05$ ) in size of lyophilized form of formulation and zeta potential as well. Water content of the lyophilized cakes was not affected during the storage period ( $p < 0.05$ ). Stability studies at accelerated and refrigerated conditions demonstrate that the product was stable at both conditions for a period of 3 months and suggest that the product will be stable for longer periods at refrigerated conditions (Figure 5.28, Table 5.28 and Table 5.29). Moreover, the liquid state form was stable till two-month time point at  $2-8^\circ\text{C}$ , thus indicating that the even after reconstitution, the formulation could maintain desired characteristic for administration. Thus, lyophilized form can be proposed as drug product presentation for shelf-storage of the developed formulation.

**Table 5.28 Stability Testing Data of DLPLs (Suspension form)**

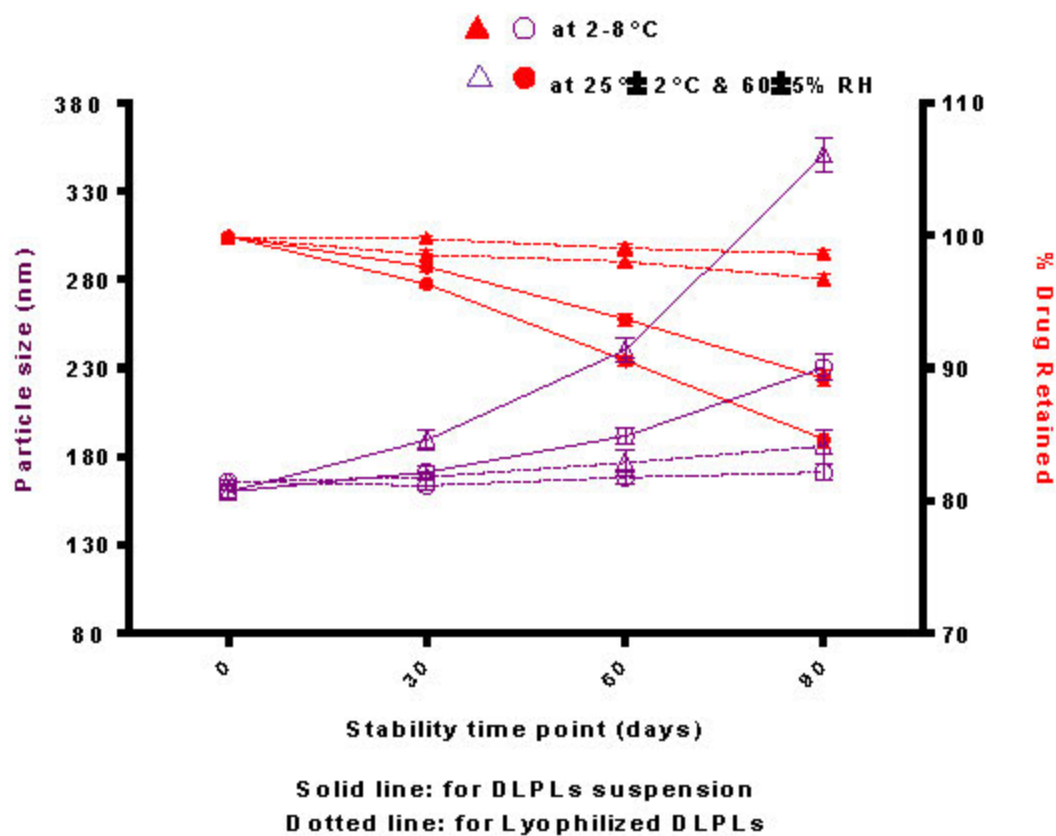
Storage condition	Time (Month)	Description	Drug Retained (%)	Particle Size (nm)	Mean Polydispersity index	Zeta potential (mV)
Initial		Translucent liquid	99.91 $\pm$ 0.12	160 $\pm$ 3.4	0.015	-3.1 $\pm$ 0.8
2-8 $^\circ\text{C}$	1	Translucent liquid	97.62 $\pm$ 0.33	171.2 $\pm$ 2.9	0.059	-3.5 $\pm$ 1.4
2-8 $^\circ\text{C}$	2	Translucent liquid	93.68 $\pm$ 0.47	191.6 $\pm$ 4.3	0.088	-2.3 $\pm$ 0.9
2-8 $^\circ\text{C}$	3	Translucent liquid	89.23 $\pm$ 0.61	230.5 $\pm$ 7.2	0.152	-2.5 $\pm$ 1.6
25 $^\circ\text{C}$ /60% RH	1	Translucent liquid	96.33 $\pm$ 0.23	189.5 $\pm$ 5.6	0.198	-4.6 $\pm$ 1.1
25 $^\circ\text{C}$ /60% RH	2	Translucent liquid	90.54 $\pm$ 0.32	240.4 $\pm$ 6.8	0.246	+0.5 $\pm$ 0.6
25 $^\circ\text{C}$ /60% RH	3	Translucent liquid	84.62 $\pm$ 0.64	350.8 $\pm$ 9.6	0.310	-0.8 $\pm$ 1.1

\*Experiments were performed in triplicate

Table 5.29 Stability Testing Data of DLPLs (Lyophilized form after reconstitution)

Storage condition	Time (Month)	Description	Assay (%)	Water content (%)	Particle size (nm)	Polydispersity index	Zeta potential (mV)
Initial (Before lyophilization)		NA	99.88±0.05	NA	160.2±3.9	0.189	-6.2±2.9
Initial (After lyophilization)		White lyophilized cake	99.84±0.09	1.36±0.49	165.6±1.5	0.185	19.6±2.1
2-8°C	1	White lyophilized cake	99.76±0.25	1.39±0.51	166.6±2.9	0.189	20.1±3.2
2-8°C	2	White lyophilized cake	99.04±0.34	1.45±0.43	168.2±4.3	0.198	16.5±1.6
2-8°C	3	White lyophilized cake	98.63±0.32	1.59±0.29	171.0±4.2	0.192	17.2±2.0
25°C/60% RH	1	White lyophilized cake	98.56±0.36	1.32±0.43	168.3±2.1	0.186	18.4±2.2
25°C/60% RH	2	White lyophilized cake	98.05±0.4	1.30±0.31	176.4±6.8	0.201	19.2±2.8
25°C/60% RH	3	White lyophilized cake	96.72±0.38	1.28±0.30	185.8±9.6	0.195	19.6±1.6

\*Experiments were performed in triplicate



\*Experiments were performed in triplicate

Figure 5.28 Stability study results for PLs and DLPLs

## 5.5 References

1. Sharma A, Sharma US. Liposomes in drug delivery: Progress and limitations. *International Journal of Pharmaceutics*. 1997;154(2):123-40.
2. Lasic DD. *Liposomes: from physics to applications*: Elsevier, 1993.
3. Surapaneni MS, Das SK, Das NG. Designing Paclitaxel drug delivery systems aimed at improved patient outcomes: current status and challenges. *ISRN pharmacology*. 2012;2012:623139.
4. Huwyler J, Drewe J, Krähenbühl S. Tumor targeting using liposomal antineoplastic drugs. *International Journal of Nanomedicine*. 2008;3(1):21-9.
5. Rowinsky EK, Donehower RC. Paclitaxel (taxol). *The New England journal of medicine*. 1995;332(15):1004-14.
6. Cheon Lee S, Kim C, Chan Kwon I, Chung H, Young Jeong S. Polymeric micelles of poly(2-ethyl-2-oxazoline)-block-poly( $\epsilon$ -caprolactone) copolymer as a carrier for paclitaxel. *Journal of Controlled Release*. 2003;89(3):437-46.
7. Feng X, Yuan Y-J, Wu J-C. Synthesis and evaluation of water-soluble paclitaxel prodrugs. *Bioorganic & Medicinal Chemistry Letters*. 2002;12(22):3301-3.
8. Dosio F, Arpicco S, Brusa P, Stella B, Cattel L. Poly(ethylene glycol)-human serum albumin-paclitaxel conjugates: preparation, characterization and pharmacokinetics. *Journal of controlled release : official journal of the Controlled Release Society*. 2001;76(1-2):107-17.
9. Liu C, Strobl JS, Bane S, Schilling JK, McCracken M, Chatterjee SK, et al. Design, synthesis, and bioactivities of steroid-linked taxol analogues as potential targeted drugs for prostate and breast cancer. *Journal of natural products*. 2004;67(2):152-9.
10. Lundberg BB, Risovic V, Ramaswamy M, Wasan KM. A lipophilic paclitaxel derivative incorporated in a lipid emulsion for parenteral administration. *Journal of controlled release : official journal of the Controlled Release Society*. 2003;86(1):93-100.
11. Ruan G, Feng SS. Preparation and characterization of poly(lactic acid)-poly(ethylene glycol)-poly(lactic acid) (PLA-PEG-PLA) microspheres for controlled release of paclitaxel. *Biomaterials*. 2003;24(27):5037-44.

12. Sharma US, Balasubramanian SV, Straubinger RM. Pharmaceutical and physical properties of paclitaxel (Taxol) complexes with cyclodextrins. *J Pharm Sci*. 1995;84(10):1223-30.
13. Merisko-Liversidge E, Sarpotdar P, Bruno J, Hajj S, Wei L, Peltier N, et al. Formulation and antitumor activity evaluation of nanocrystalline suspensions of poorly soluble anticancer drugs. *Pharmaceutical research*. 1996;13(2):272-8.
14. Soepenbergh O, Sparreboom A, de Jonge MJ, Planting AS, de Heus G, Loos WJ, et al. Real-time pharmacokinetics guiding clinical decisions; phase I study of a weekly schedule of liposome encapsulated paclitaxel in patients with solid tumours. *European journal of cancer (Oxford, England : 1990)*. 2004;40(5):681-8.
15. Strieth S, Nussbaum CF, Eichhorn ME, Fuhrmann M, Teifel M, Michaelis U, et al. Tumor-selective vessel occlusions by platelets after vascular targeting chemotherapy using paclitaxel encapsulated in cationic liposomes. *International journal of cancer*. 2008;122(2):452-60.
16. Christopheit M, Lenz G, Forstpointner R, Bartelheim K, Kuhnbach R, Naujoks K, et al. Nine months to progression using fourth-line liposomally encapsulated paclitaxel against hepatocellular carcinoma. *Chemotherapy*. 2008;54(4):309-14.
17. Garber K. Improved Paclitaxel formulation hints at new chemotherapy approach. *Journal of the National Cancer Institute*. 2004;96(2):90-1.
18. Gradishar WJ, Tjulandin S, Davidson N, Shaw H, Desai N, Bhar P, et al. Phase III trial of nanoparticle albumin-bound paclitaxel compared with polyethylated castor oil-based paclitaxel in women with breast cancer. *Journal of clinical oncology : official journal of the American Society of Clinical Oncology*. 2005;23(31):7794-803.
19. Koo H, Min KH, Lee SC, Park JH, Park K, Jeong SY, et al. Enhanced drug-loading and therapeutic efficacy of hydrotropic oligomer-conjugated glycol chitosan nanoparticles for tumor-targeted paclitaxel delivery. *Journal of controlled release : official journal of the Controlled Release Society*. 2013;172(3):823-31.
20. Fracasso PM, Picus J, Wildi JD, Goodner SA, Creekmore AN, Gao F, et al. Phase I and pharmacokinetic study of weekly docosahexaenoic acid-paclitaxel, Taxoprexin, in resistant solid tumor malignancies. *Cancer chemotherapy and pharmacology*. 2009;63(3):451-8.

21. Homsí J, Bedikian AY, Papadopoulos NE, Kim KB, Hwu WJ, Mahoney SL, et al. Phase 2 open-label study of weekly docosahexaenoic acid-paclitaxel in patients with metastatic uveal melanoma. *Melanoma research*. 2010;20(6):507-10.
22. Wang H, Wu Y, Zhao R, Nie G. Engineering the assemblies of biomaterial nanocarriers for delivery of multiple theranostic agents with enhanced antitumor efficacy. *Advanced materials (Deerfield Beach, Fla)*. 2013;25(11):1616-22.
23. Northfelt DW, Allred JB, Liu H, Hobday TJ, Rodacker MW, Lyss AP, et al. Phase 2 trial of paclitaxel polyglumex with capecitabine for metastatic breast cancer. *American journal of clinical oncology*. 2014;37(2):167-71.
24. Kurzrock R, Gabrail N, Chandhasin C, Moulder S, Smith C, Brenner A, et al. Safety, pharmacokinetics, and activity of GRN1005, a novel conjugate of angiopep-2, a peptide facilitating brain penetration, and paclitaxel, in patients with advanced solid tumors. *Molecular cancer therapeutics*. 2012;11(2):308-16.
25. von Euler H, Rivera P, Nymán H, Haggström J, Borga O. A dose-finding study with a novel water-soluble formulation of paclitaxel for the treatment of malignant high-grade solid tumours in dogs. *Veterinary and comparative oncology*. 2013;11(4):243-55.
26. Hendricks WP, Yang J, Sur S, Zhou S. Formulating the magic bullet: barriers to clinical translation of nanoparticle cancer gene therapy. *Nanomedicine (London, England)*. 2014;9(8):1121-4.
27. Maestrelli F, Gonzalez-Rodriguez ML, Rabasco AM, Mura P. Preparation and characterisation of liposomes encapsulating ketoprofen-cyclodextrin complexes for transdermal drug delivery. *Int J Pharm*. 2005;298(1):55-67.
28. Zhang L, Zhang Q, Wang X, Zhang W, Lin C, Chen F, et al. Drug-in-cyclodextrin-in-liposomes: A novel drug delivery system for flurbiprofen. *Int J Pharm*. 2015;492(1-2):40-5.
29. Chen J, Lu WL, Gu W, Lu SS, Chen ZP, Cai BC, et al. Drug-in-cyclodextrin-in-liposomes: a promising delivery system for hydrophobic drugs. *Expert opinion on drug delivery*. 2014;11(4):565-77.
30. McCormack B, Gregoriadis G. Entrapment of cyclodextrin-drug complexes into liposomes: potential advantages in drug delivery. *Journal of drug targeting*. 1994;2(5):449-54.

31. Luo LM, Huang Y, Zhao BX, Zhao X, Duan Y, Du R, et al. Anti-tumor and anti-angiogenic effect of metronomic cyclic NGR-modified liposomes containing paclitaxel. *Biomaterials*. 2013;34(4):1102-14.
32. Ducat E, Brion M, Lecomte F, Evrard B, Piel G. The experimental design as practical approach to develop and optimize a formulation of peptide-loaded liposomes. *AAPS PharmSciTech*. 2010;11(2):966-75.
33. Naik S, Patel D, Surti N, Misra A. Preparation of PEGylated liposomes of docetaxel using supercritical fluid technology. *The Journal of Supercritical Fluids*. 2010;54(1):110-9.
34. Singh B, Dahiya M, Saharan V, Ahuja N. Optimizing drug delivery systems using systematic "design of experiments." Part II: retrospect and prospects. *Critical reviews in therapeutic drug carrier systems*. 2005;22(3):215-94.
35. Xiong Y, Guo D, Wang L, Zheng X, Zhang Y, Chen J. Development of nobiletin loaded liposomal formulation using response surface methodology. *International journal of pharmaceutics*. 2009;371(1-2):197-203.
36. Stensrud G, Sande SA, Kristensen S, Smistad G. Formulation and characterisation of primaquine loaded liposomes prepared by a pH gradient using experimental design. *International journal of pharmaceutics*. 2000;198(2):213-28.
37. Singh B, Mehta G, Kumar R, Bhatia A, Ahuja N, Katare OP. Design, development and optimization of nimesulide-loaded liposomal systems for topical application. *Current drug delivery*. 2005;2(2):143-53.
38. Armstrong NA, James KC. *Understanding Experimental Designs and Interpretation in Pharmaceutics*. London: Ellis Horwood; 1990.
39. Box GEP, Hunter WG, Hunger JS. *Statistics for Experimenters*. New York: Wiley; 1978.
40. Mak KWY, Yap MGS, Teo WK. Formulation and optimization of two culture media for the production of tumour necrosis factor- $\beta$  in *Escherichia coli*. *Journal of Chemical Technology & Biotechnology*. 1995;62(3):289-94.
41. Box GEP, Wilson KB. On the Experimental Attainment of Optimum Conditions. *Journal of the Royal Statistical Society Series B (Methodological)*. 1951;13(1):1-45.

42. Qiu N, Cai L, Wang W, Wang G, Cheng X, Xu Q, et al. Barbigerone-in-hydroxypropyl- $\beta$ -cyclodextrin-liposomal nanoparticle: preparation, characterization and anti-cancer activities. *Journal of Inclusion Phenomena and Macrocyclic Chemistry*. 2015;82(3):505-14.
43. Zhang C, Qineng P, Zhang H. Self-assembly and characterization of paclitaxel-loaded N-octyl-O-sulfate chitosan micellar system. *Colloids and surfaces B, Biointerfaces*. 2004;39(1-2):69-75.
44. Yang T, Cui FD, Choi MK, Cho JW, Chung SJ, Shim CK, et al. Enhanced solubility and stability of PEGylated liposomal paclitaxel: in vitro and in vivo evaluation. *International journal of pharmaceutics*. 2007;338(1-2):317-26.
45. M. Badr-Eldin S, A. Ahmed T, R Ismail H. Aripiprazole-Cyclodextrin Binary Systems for Dissolution Enhancement: Effect of Preparation Technique, Cyclodextrin Type and Molar Ratio. *Iranian Journal of Basic Medical Sciences*. 2013;16(12):1223-31.
46. Moyano JR, Ginés JM, Arias MJ, Rabasco AM. Study of the dissolution characteristics of oxazepam via complexation with  $\beta$ -cyclodextrin. *International journal of pharmaceutics*. 1995;114(1):95-102.
47. Cacela C, Hinch DK. Low Amounts of Sucrose Are Sufficient to Depress the Phase Transition Temperature of Dry Phosphatidylcholine, but Not for Lyoprotection of Liposomes. *Biophysical Journal*. 2006;90(8):2831-42.
48. Wulff M, Alden M. Solid state studies of drug-cyclodextrin inclusion complexes in PEG 6000 prepared by a new method. *European journal of pharmaceutical sciences : official journal of the European Federation for Pharmaceutical Sciences*. 1999;8(4):269-81.
49. Fakes MG, Dali MV, Haby TA, Morris KR, Varia SA, Serajuddin AT. Moisture sorption behavior of selected bulking agents used in lyophilized products. *PDA journal of pharmaceutical science and technology / PDA*. 2000;54(2):144-9.
50. Crowe LM, Crowe JH, Rudolph A, Womersley C, Appel L. Preservation of freeze-dried liposomes by trehalose. *Archives of biochemistry and biophysics*. 1985;242(1):240-7.
51. Talsma H, Crommelin DJ. Liposomes as Drug Delivery Systems, Part III: Stabilization. *Pharmaceutucial Technology*. 1992;17:48-59.

52. Grit M, Crommelin DJ. The effect of aging on the physical stability of liposome dispersions. *Chemistry and physics of lipids*. 1992;62(2):113-22.
53. Cliff RO, Ligler F, Goins B, Hoffmann PM, Spielberg H, Rudolph AS. Liposome encapsulated hemoglobin: long-term storage stability and in vivo characterization. *Biomaterials, artificial cells, and immobilization biotechnology: official journal of the International Society for Artificial Cells and Immobilization Biotechnology*. 1992;20(2-4):619-26.
54. Fang JY, Lin HH, Hsu LR, Tsai YH. Characterization and stability of various liposome-encapsulated enoxacin formulations. *Chemical & pharmaceutical bulletin*. 1997;45(9):1504-9.
55. Slabbert C, Plessis LH, Kotze AF. Evaluation of the physical properties and stability of two lipid drug delivery systems containing mefloquine. *International journal of pharmaceutics*. 2011;409(1-2):209-15.
56. Frokjaer S, Hjorth EL, Worts O. Stability testing of liposomes during storage. In: Gregoriadis G, editor. *Liposome Technology: Preparation of Liposomes*. Boca Raton, Florida, US: CRC Press; 1984. p. 235-45.
57. Singh S. Drug stability testing and shelf-life determination according to international guidelines. *Pharm Technol*. 1999;23:68-88.
58. US FDA (CDER), Draft Guidance for Industry Liposome Drug Products. CMC Documentation.
59. Ugwu S, Zhang A, Parmar M, Miller B, Sardone T, Peikov V, et al. Preparation, characterization, and stability of liposome-based formulations of mitoxantrone. *Drug development and industrial pharmacy*. 2005;31(2):223-9.
60. Winterhalter M, Lasic DD. Liposome stability and formation: experimental parameters and theories on the size distribution. *Chemistry and physics of lipids*. 1993;64(1-3):35-43.
61. Changsan N, Chan HK, Separovic F, Srichana T. Physicochemical characterization and stability of rifampicin liposome dry powder formulations for inhalation. *Journal of pharmaceutical sciences*. 2009;98(2):628-39.

62. Yang T, Cui FD, Choi MK, Lin H, Chung SJ, Shim CK, et al. Liposome formulation of paclitaxel with enhanced solubility and stability. *Drug delivery*. 2007;14(5):301-8.
63. Anderson M, Omri A. The effect of different lipid components on the in vitro stability and release kinetics of liposome formulations. *Drug delivery*. 2004;11(1):33-9.
64. Manosroi A, Podjanasoonthon K, Manosroi J. Stability and release of topical tranexamic acid liposome formulations. *Journal of cosmetic science*. 2002;53(6):375-86.
65. Manosroi A, Kongkanermit L, Manosroi J. Characterization of amphotericin B liposome formulations. *Drug development and industrial pharmacy*. 2004;30(5):535-43.
66. Bhalerao SS, Raje Harshal A. Preparation, optimization, characterization, and stability studies of salicylic acid liposomes. *Drug development and industrial pharmacy*. 2003;29(4):451-67.
67. van Hoogevest P, Wendel A. The use of natural and synthetic phospholipids as pharmaceutical excipients. *European Journal of Lipid Science and Technology*. 2014;116(9):1088-107.
68. Hinrichs WL, Mancenido FA, Sanders NN, Braeckmans K, De Smedt SC, Demeester J, et al. The choice of a suitable oligosaccharide to prevent aggregation of PEGylated nanoparticles during freeze thawing and freeze drying. *International journal of pharmaceutics*. 2006;311(1-2):237-44.
69. Anchoroquy TJ, Girouard LG, Carpenter JF, Kroll DJ. Stability of lipid/DNA complexes during agitation and freeze-thawing. *Journal of Pharmaceutical Sciences*. 1998;87(9):1046-51.
70. Anchoroquy TJ, Koe GS. Physical stability of nonviral plasmid-based therapeutics. *Journal of Pharmaceutical Sciences*. 2000;89(3):289-96.
71. Armstrong TK, Anchoroquy TJ. Immobilization of nonviral vectors during the freezing step of lyophilization. *Journal of Pharmaceutical Sciences*. 2004;93(11):2698-709.
72. Crowe JH, Leslie SB, Crowe LM. Is vitrification sufficient to preserve liposomes during freeze-drying? *Cryobiology*. 1994;31(4):355-66.
73. Allison SD, Anchoroquy TJ. Mechanisms of protection of cationic lipid-DNA complexes during lyophilization. *Journal of Pharmaceutical Sciences*. 2000;89(5):682-91.

74. Allison SD, Molina MC, Anchoroquy TJ. Stabilization of lipid/DNA complexes during the freezing step of the lyophilization process: the particle isolation hypothesis. *Biochimica et biophysica acta*. 2000;1468(1-2):127-38.
75. Molina MC, Allison SD, Anchoroquy TJ. Maintenance of nonviral vector particle size during the freezing step of the lyophilization process is insufficient for preservation of activity: insight from other structural indicators. *J Pharm Sci*. 2001;90(10):1445-55.
76. Vhora I, Khatri N, Desai J, Thakkar HP. Caprylate-conjugated Cisplatin for the development of novel liposomal formulation. *AAPS PharmSciTech*. 2014;15(4):845-57.
77. Khatri N, Baradia D, Vhora I, Rathi M, Misra A. Development and characterization of siRNA lipoplexes: Effect of different lipids, in vitro evaluation in cancerous cell lines and in vivo toxicity study. *AAPS PharmSciTech*. 2014;15(6):1630-43.
78. Fildes F. Liposomes: The Industrial view point. In: *Liposomes from Physical Structure to Therapeutic Applications*. Knight C, editor. New York, US: Elsevier Biomedical Press; 1998.